AD NUMBER

ADB097999

NEW LIMITATION CHANGE

TO

Approved for public release, distribution unlimited

FROM

Distribution authorized to U.S. Gov't. agencies only; Test and Evaluation; NOV 1985. Other requests shall be referred to Army Armament Research and Development Center, Attn: SMCAR-MSI, Dover,NJ 07801-5001.

AUTHORITY

USAARDCOM, via ltr, 30 Jul 1986

AD D 97999

AUTHORITY
ISAAC [illegible] L-1
30 Jul 66

TECHNICAL REPORT ARAED-TR-85004

DYNAMIC AND QUASI STATIC MECHANICAL PROPERTIES OF COMP B AND TNT

J. PINTO
S. NICOLAIDES
D. A. WEIGAND

NOVEMBER 1985

US ARMY ARMAMENT MUNITIONS & CHEMICAL COMMAND
ARMAMENT R&D CENTER

U. S. ARMY ARMAMENT RESEARCH AND DEVELOPMENT CENTER
ARMAMENT ENGINEERING DIRECTORATE
DOVER, NEW JERSEY

UNCLASSIFIED

SECURITY CLASSIFICATION OF THIS PAGE (When Data Entered)

REPORT DOCUMENTATION PAGE

READ INSTRUCTIONS BEFORE COMPLETING FORM

1 REPORT NUMBER: Technical Report ARAED-TR-85004

2 GOVT ACCESSION NO: AD-A161996

3 RECIPIENT'S CATALOG NUMBER

4 TITLE (and Subtitle): DYNAMIC AND QUASI STATIC MECHANICAL PROPERTIES OF COMP B AND TNT

5 TYPE OF REPORT & PERIOD COVERED

6 PERFORMING ORG. REPORT NUMBER

7 AUTHOR(s): J. Pinto, S. Nicolaides, and D.A. Weigand

8 CONTRACT OR GRANT NUMBER(s)

9 PERFORMING ORGANIZATION NAME AND ADDRESS: ARDC, AED
Energetics and Warheads Div (SMCAR-AEE)
Dover, NJ 07801-5001

10 PROGRAM ELEMENT, PROJECT, TASK AREA & WORK UNIT NUMBERS: 7518-03-010

11 CONTROLLING OFFICE NAME AND ADDRESS: ARDC, IMD
STINFO, Div (SMCAR-MSI)
Dover, NJ 07801-5001

12 REPORT DATE: November 1985

13 NUMBER OF PAGES: 64

14 MONITORING AGENCY NAME & ADDRESS (if different from Controlling Office)

15 SECURITY CLASS. (of this report): Unclassified

15a DECLASSIFICATION/DOWNGRADING SCHEDULE

16 DISTRIBUTION STATEMENT (of this Report)

DTIC

Distribution limited to U.S. Government agencies only; [redacted]; November 1985. Other requests for this document must be referred to ARDC, ATTN: SMCAR-MSI, Dover, NJ 07801-5001.

17 DISTRIBUTION STATEMENT (of the abstract entered in Block 20, if different from Report)

18 SUPPLEMENTARY NOTES

This project was initiated in 1980 by the Large Caliber Weapon Systems Laboratory, Energetic Materials Division, ARDC.

19 KEY WORDS (Continue on reverse side if necessary and identify by block number)

Yield strength	Strain rate	Stress
Compressive strength	Composition B	Strain
von Mises yield strength	TNT	Mechanical properties
Uniaxial compression	Friction	Dynamic

(continued)

20 ABSTRACT (Continue on reverse side if necessary and identify by block number)

Studies have been made of the mechanical properties of Composition B and TNT cast from the melt. Measurements were made in uniaxial compression and triaxial compression (uniaxial strain) as a function of temperature and strain rate. The mechanical properties have been investigated at low quasi static

(continued)

DD FORM 1 JAN 73 1473 EDITION OF 1 NOV 65 IS OBSOLETE

UNCLASSIFIED

SECURITY CLASSIFICATION OF THIS PAGE (When Data Entered)

19. KEY WORDS (CONTINUED)

Quasi static
RDX particle size
Wax
Porosity
Poisson's ratio
Elastic constants
Plastic
Load cell
Graphite powder
Viscosity
Thermal strains
TNT puriety
Brittle
Artillery launch
Cracks
Thermal expansion
Servo-hydraulic
Strain gages
Split mold
Explosives
TNT puriety
Voids
Young's modulus
Tiaxial loading
Elastic
LVDT
Thermocouple
Cyclotol

20. ABSTRACT (CONTINUED)

strain rates and at dynamic (failure in 2 to 10 milliseconds) stain rates to simulate gun launch conditions. The quasi static results will be used to model conditions as the material is cooled from the melt and the dynamic results will be available to model the response to gun launch conditions. Two variations of Composition B were also studied in which the TNT purity, the RDX particle size, and the wax content were varied.

The results indicate that Comp B is stronger and stiffer than TNT for all conditions of measurements used. In addition, the yield strength under the confined condition of the triaxial test is larger than the uniaxial compressive strength as expected for brittle materials. Both the yield strength and the compressive strength decrease with increasing temperature and decreasing strain rate. The results are discussed in terms of known mechanisms of mechanical failure.

CONTENTS

TABLES

FIGURES

INTRODUCTION

The mechanical properties of Composition B (Comp B) and trinitrotoluene (TNT) have been studied in compression as a function of temperature at two strain rate . Trinitrotoluene is an organic polycrystalline solid, and Comp B is a composite of TNT and cyclotrimethylene trinitramine (RDX), RDX also being a polycrystalline solid of higher melting temperature than TNT. Comp B is made up of 39.4% TNT, 59.6% RDX, and 1% wax. Both Comp B and TNT can be loaded by casting from the melt (TNT). The mechanical properties of both explosives are needed to understand these materials, to model the thermal strains etc., introduced on cooling from melt, and also to model the behavior during artillery launch conditions. Quasi static measurements have been made to obtain the parameters needed for modeling the explosives as they cool from the melt and dynamic medium rate measurements have been made to obtain parameters in the artillery launch time frame. The elastic constants are needed for modeling and, in addition, the failure criteria, e.g. the uniaxial compressive strengths, are needed. Mechanical failure can lead to crack and void formation in the quasi static time frame and this can lead to ignition and prematures in the dynamic time frame. Some calculations have already been made for the launch time frame using the available elastic constants and failure criteria. However, no one has calculated the thermal strain introduced on cooling from the melt. Calculations will be made to determine the best condition for cooling from the melt to give the minimum amount of thermal strain induced by cooling and thus give the best cast.

The mechanical properties of Comp B have also been studied as a function of composition in an effort to determine the effects of changes in composition. Thus, studies have been made as a function of RDX particle size, TNT purity and with and without wax. Measurements have been made of TNT both for a reference for Comp B and because TNT is an important explosive itself.

Composition B and TNT are very brittle materials and are much weaker in tension than compression. In addition, these materials fail at a lower value of stress if they are unconfined than if they are confined. Thus, measurements have been made to obtain the uniaxial compressive strengths (unconfined) and the triaxial yield strengths (confined) to place limits on the failure criteria. Because of voids and porosity in the casts, there are free surfaces to fail. Measurements were made as a function of temperature at a higher rate resulting in failure in 2 to 10 milliseconds so as to obtain information for the modeling of the explosive during artillery launch.

BACKGROUND

Uniaxial

The mechanical properties of Comp B and of TNT loaded uniaxially in compression were measured as a function of temperature and strain rate. Although lubrication was used to minimize friction between the sample ends and the cross heads,

which applied compressional loading, frictional forces could only be minimized. Thus, the stresses are not strictly uniaxial especially near the sample ends. However, as a first approximation the state of stress is referred to in the following as uniaxial. The effects of frictional stress on the sample ends is also considered in the Discussion Section.

In unaxial compression these materials fail in a brittle manner. The compressive strength is the stress at which this brittle failure occurs, and it appears as a maximum on the stress versus strain curve (see fig. 1). The strain which corresponds to this peak stress is also reported. The stress versus strain curves for these materials are temperature and rate dependent but generally consist of an initial straight line portion. The slope of this initial portion of the curve was taken as Young's modulus (see fig. 1).

Triaxial

The uniaxial compressive strength of these brittle materials is apparently dependent on flaws such as cracks or voids where stress concentrations can develop and failure apparently takes place by crack propagation. This type of brittle failure is not observed if crack propagation is hindered by triaxial confinement (see fig. 3) and experimental techniques have been used to determine the mechanical properties of brittle materials under triaxial loading (ref 1). By using triaxial loading, it is possible to determine the yield strength, in addition to the elastic constants, and one type of triaxial loading has been used to study Comp B, TNT, and other similar materials over a range of temperatures and strain rates (ref 2). The same general experimental techniques are used in this work.

The stress strain relationships can be written as:

$$\epsilon_i = \sum_{ij} S_{ij} \sigma_j \qquad (1)$$

where the ϵ_i are the strains, σ_j are the stresses and S_{ij} are the elastic compliances. For triaxial loading normal to the surface in three orthogonal directions taken as the x, y, and z axes and for an isotopic material, equations 1 reduce to:

$$\epsilon_x = S_{11}\sigma_x + S_{12}\sigma_y + S_{12}\sigma_z \qquad (2a)$$

$$\epsilon_y = S_{12}\sigma_x + S_{11}\sigma_y + S_{12}\sigma_z \qquad (2b)$$

$$\epsilon_z = S_{12}\sigma_x + S_{12}\sigma_y + S_{11}\sigma_z \qquad (2c)$$

where it can be shown that Young's modulus E and Poisson's ration ν are:

$$E = 1/S_{11} \tag{3a}$$

$$\nu = -S_{12}/S_{11}$$

The sign convention taken here is that ν is a positive number. For the triaxial experimental procedure used here, a cylindrically shaped specimen is enclosed in a close fitting, thick-wall steel tube and compressed along the z axis as shown in figure 2. A tight fit between the specimen and the steel tube is obtained by increasing the temperature a few degrees until a hoop strain is observed on the outer wall of the steel tube. This occurs because the sample has a higher coefficient of thermal expansion than the steel. Since the steel tube is much stiffer than the test specimen, the strains in the x and y direction are negligible. Also, from cylindrical symmetry:

$$\sigma_x = \sigma_y = \sigma_R \tag{4}$$

Using this identity and $\varepsilon_x = \varepsilon_y = 0$ equation (5) is obtained from either equation 2a or 2b.

$$\sigma_R = \frac{\nu}{1-\nu}\ \sigma_A \tag{5}$$

where $\sigma_A = \sigma_z$. This equation shows that the slope of the radial stress versus axial stress curve in the elastic region is determined by Poisson's ratio (see fig. 3). Solving for ν in terms of this slope m gives:

$$\nu = \frac{m}{1+m} \tag{6}$$

where $m = d\sigma_R/d\sigma_A$

Furthermore, if we substitute equation 3 into equation 2c, use equations 4 and 5, and solve for the elastic modulus, we obtain

$$E = \frac{\sigma_z}{\varepsilon_z}\ \left[1 - \frac{2\nu}{1-\nu}^2\right] \tag{7}$$

Thus, after obtaining ν from the slope of the σ_R versus σ_A curve, the modulus can be obtained from the slope of the axial (z direction) stress versus strain curve (see fig. 4).

These equations apply to a material which is in an elastic state of stress. Under continued action of an applied axial stress the material will eventually

undergo a transition from an elastic to a plastic state. This transition is characterized by a yield point. Various criteria can be used to determine yield. The von Mises criteria is used here, and can be stated as follows (ref 1):

$$Y = \frac{1}{2^{1/2}} \left[(\sigma_x - \sigma_y)^2 + (\sigma_x - \sigma_z)^2 + (\sigma_y - \sigma_z)^2\right]^{1/2} \quad (8)$$

where Y is the yield strength. Using equation 4, this reduces to

$$Y = \sigma_A - \sigma_R \quad (9)$$

These considerations indicate that the radial versus axial stress curve will have a break, with the initial or elastic region being determined by equation 5 and the yield region determined by equation 9 (see fig. 3). Under ideal circumstances the yield strength can be found by taking the difference between σ_A and σ_R anywhere along the curve after the transition has occurred. In the work reported here, the yield strength, Y, was taken as the intercept on the σ_A axis of the straight line portion of the σ_R versus σ_A curve given by equation 9.

EXPERIMENTAL

Loading Apparatus

The mechanical properties experiments described in this report were performed using a medium rate, high load, servo-hydraulic system assembled for this installation by the MTS Corporation. A schematic of the system is shown in figure 5. A compressive or tensile load can be applied to a test specimen by hydraulically moving the actuator rod up or down. The system can apply a force of up to 35,000 pounds and can achieve a maximum free run velocity of up to 4,800 inches per minute. Strain rates in the range up to 10/sec can be obtained for explosive samples of the size used in this work. Failure of a test specimen can be achieved in approximately 2 to 5 milliseconds.

The operation of the apparatus is controlled by a PDP 11/03 microcomputer, with a memory of 16K available for running programs. A dual drive floppy disk system is also available providing an additional 228K of memory for data and program storage. Any desired load-time, displacement-time, or strain-time profile within the limits of the system can be programmed into the computer and applied to a test specimen. The computer also controls data acquisition, data analysis, data display, hard copy generation, and data transfer to the mass storage device. The electronics and control parts of the apparatus are isolated physically from the part of the system that loads the test specimen such that explosives and propellants can be tested safely.

A linear variable differential transformer (LVDT) measures the displacement of the actuator rod and a load cell is used to measure the applied force. Amplifiers are available for three sets of strain gage circuits. Compressive or tensile loads can be applied to a test specimen using appropriate grips and fixtures. The compression platens and tensile fixtures are enclosed in a large insulated chamber for temperature conditioning. The air in this chamber is either heated electrically or cooled by blowing solid carbon dioxide into the chamber. A control thermocouple regulates the flow of current to the heater or of coolant into the chamber to achieve and maintain the desired temperature.

Uniaxial Experiments

In order to measure uniaxial compressive properties of Comp B and TNT, cylindrically shaped test specimens are first coated on their end faces with a thin film of graphite powder in order to minimize binding and friction at the compression faces. The test specimens are placed on the top face of the actuator rod for temperature conditioning. Thermocouples are attached to the top and bottom of each specimen, and a thermocouple is suspended in the air right next to the specimen. These temperatures are monitored until equilibrium at the desired test temperature is achieved. For extremely high temperatures heating tape is wrapped around the metal parts to bring them to the desired temperature more quickly.

When the desired test temperature is achieved the test specimen is slowly brought into contact with the upper platen. A small pre-stress of approximately 50 psi is applied to the specimen. A displacement versus time profile is then programmed into the computer and applied to the test specimen.

Triaxial Experiments

The experimental arrangement for measuring the yield strength under radial confinement is shown in figure 2. The confining test cylinder is made of hardened steel. The length of the cylinder is 4.9 inches, the inner diameter is 0.752 inches, and the thickness of the cell wall is 0.5 inches. The upper and lower anvils are also made of hardened steel. The confining cylinder sits on a base made of hard rubber. The lengths of the anvils and the thickness of the base are chosen such that the test specimen sits in the middle of the cell.

SR-4 strain gages are glued to the outside of the test cell to measure the hoop strain. The hoop strain is related to the internal pressure exerted by the test specimen on the steel cell by the equation

$$\sigma_R = \frac{E\,(b^2 - a^2)}{2a^2} \cdot \varepsilon_R \qquad (10)$$

where a and b are the inner and outer radii of the test cell, E is the elastic modulus of the test cell material, ε_R is the hoop strain, and σ_R is the radial stress exerted by the test specimen on the test cell.

A tight fit must exist between the test specimen and the walls of the test cell. Since it is necessary to measure these properties as a function of temperature, test specimens were machined to a variety of diameters near 0.752 inches. Then, by calculating a dimensional change for a specified temperature change, a specimen of the proper diameter can be chosen, placed in the test cell, and heated to the desired test temperature in the conditioning box. Since the thermal coefficients of expansion of Comp B and TNT are greater that that of steel, this procedure enables the test specimen to come into contact with the walls of the steel test cell. Thermocouples are attached to various locations on the test cell, on the anvils, and on the metal parts in contact with the test fixture. The experiment is carried out when all of the thermocouples indicate that thermal equilibrium has been attained.

In order to minimize binding and friction inside the test cell, the entire test specimen is coated with a thin film of graphite powder before being placed in the cell. The effects of friction on the measured yield strength and elastic constants are discussed below in another section.

When the test cell and test specimen reach thermal equilibrium at the desired temperature, the test fixture is brought into contact with the upper platen and a load versus time profile is programmed into the computer and applied to the specimen.

At low rates the apparatus is capable of applying a constant load or displacement rate. At such rates, the initial acceleration is not significant. However, when the apparatus is driven to its maximum possible velocity, the acceleration and deceleration could be a significant portion of the total profile. In order to avoid deceleration problems, the apparatus is overdriven, i.e., a load or displacement higher than necessary to achieve yield or failure is programmed into the computer. The load or displacement versus time curve obtained from such an experiment does not have a constant slope. A typical example of a load versus time curve used in the triaxial experiments is shown in figure 6. The load rises rapidly until a plateau is reached at approximately 16,000 pounds. This profile has been designed so that the event under study i.e., yielding of the specimen, has taken place at an axial load less than the plateau value of 16,000 pounds.

Sample Preparation

Composition B and TNT casts were made by pouring the molten material (TNT) either into a 105 mm split mold (see fig. 7) or into cardboard cylinders. The casts were cut as described below and machined to the desired sample dimensions and tolerances. The material was x-ray radiographed after casting and recast or discarded if there were significant cracks, voids, or porosity. All samples were also radiographed after machining.

Composition B, as obtained from the manufacturing plant (Holston), was cast into the 105 mm split mold. Some difficulty was experienced in obtaining a "good" cast, i.e., sufficiently defect free, and this material was cast or recast several times until a cast of only borderline acceptability for mechanical properties measurements was obtained. The split mold and riser were pre-heated on a steam table, the Comp B was poured at 82°C, the filled mold was wrapped in insulation, and a steam-heated probe was inserted into the top to prevent rapid and localized solidification. Military grade TNT, as obtained from the manufacturing plant, (Volunteer) was cast with procedures similar to those for Comp B, except the pouring temperature was 76°C. In this case, the quality of the cast was poor and recasting was necessary to obtain only borderline acceptability.

In addition, two variations of Comp B type formulations were cast. These are designated Comp B I (cyclotol) and Comp B II and information on these are given in table 1. Comp B I differs from Comp B because of purified TNT and the absence of wax. Comp B II differs from Comp B because fine (Grade G) RDX was used rather than the course (Grade A) RDX. In table 1 the compositions are given including the cyclotetramethylene tetranitramine (HMX) content as determined by high pressure liquid chromatography (HPLC), as a fraction of RDX for the two lots. The particle size distribution of the RDX as determined by passage through sieves of various sizes and the melting points of the TNT are also given. Whatever purification of TNT that was accomplished by recrystallization did not influence the melting temperature.

These two forms of Comp B were cast in the 105 mm split mold following approximately the same proceedure given above for Comp B and TNT. In addition, a vacuum was applied to these melts for about 12 minutes and the filled mold of Comp B II was vibrated for 12 seconds. The pour temperature was 80° for Comp B I and 92° for Comp B II because of the higher viscosity (smaller RDX particle size). An acceptable quality cast of Comp B II was obtained on the first attempt but several attempts were necessary to obtain a borderline quality cast of Comp B I. The latter is to be excepted because of the supposedly purified TNT and the absence of wax.

The casts obtained from the split mold were cut into sections as indicated in figure 7. The sections were then further cut and machined into cylindrical samples with axes either parallel (V) to the cast axis (vertical) or perpendicular (T) to this axis (transverse). The samples were cut as shown in figure 7 and labeled according to section with a V or T as above e.g, 3V or 4T. The samples were machined into right circular cylinders 1.5 inches long with ends flat and parallel to approximately $\pm$ 0.002 inches. Samples with a range of diameters were actually obtained and these were used to make confined cylinder measurements at various temperatures.

Composition B and TNT were also cast by pouring molten explosive into cardboard cylindrical tubes both 5 inches in diameter and length and 5 inches in diameter and 13 inches in length. One sample was obtained from each of the smaller casts and the larger cast was cut up and samples prepared in much the same manner as the casts from the 105 mm split mold except that the axes of most samples obtained in this way were aligned parallel to the mold axis. In general, samples obtained in this way were of better quality than samples obtained from the split mold and the best samples were obtained from the smaller casts.

RESULTS

Composition B

Uniaxial Experiments

Standard Comp B samples, some of which were cast in the 105 mm split mold and others which were cast in smaller cardboard tubes, were measured in uniaxial compresssion. The specimens from the split mold were measured at a rate of 1.5 sec^{-1} and a temperature of 23°C to study the effects of position and orientation. The specimens from the smaller cardboard tube were measured at rates of 1.4 sec^{-1} and 6.7 x 10^{-4} sec^{-1} and at 23, 40, and 60°C. In all of these experiments axial stress and strain were measured and a modulus was calculated from the slope of the stress versus strain curve. Typical stress versus strain curves are given in figure 8 and photographs of typical sample fragments after failure are given in figures 9. The latter indicate a brittle shear type of failure. The deviation of the fracture surfaces from the 45 degree plane indicates the effect of flaws, e.g., cracks and also possible end effects, i.e. nonfrictionless contact between the crossheads and the sample surfaces.

The results of the uniaxial properties versus position and orientation are shown in table 2. One specimen each from sections two through six was measured. The orientation is indicated by a V for vertical or a T for transverse (see fig. 7). The specimen from section three had a very low compressive strength which was probably due to a flaw in the specimen. The density of this specimen was smaller than the average density for this cast but this measurement could not be repeated because the other samples from this section were used for other measurements. The properties of the other four sections show very little difference, thus suggesting that for this cast the compressive strength is independent of position and orientation. The average compressive strength is 3260 $\pm$ 150 psi, the average strain at failure is 0.65 $\pm$ 0.10%, and the average elastic modulus is (0.60 $\pm$ 0.02) x 10^6 psi. Position and orientation dependence have been found by others for low rate measurements.[1]

The results of uniaxial measurements on Comp B cast in small tubes are given in table 3 and figure 10 for two strain rates and three temperatures. The low rate compressive strength data agree well with the data of Costain and Motto (ref 3) as a function of temperature and the high rate compressive strength at 23°C is in rough agreement with the results of Clark and Schmitt (ref 2). These results indicate that the uniaxial compressive strength decreases with increasing temperature and decreasing strain rate. Clark and Schmitt also report a decreasing compressive strength with decreasing rate (ref 2).

---

[1] D. Georgevich, private communication.

Both Clark and Schmitt (ref 2) and Costain and Motto (ref 3) report moduli which are significantly larger (a factor of two or more) than values reported here at 23°C. Smaller strains at failure are also reported by these investigators. The methods of sample preparation and the quality of the samples used by these investigators are unknown. In addition, the procedures for obtaining the moduli, e.g., initial tangent or secant methods are not given. In this work the stress strain curves are linear almost to failure (see fig. 1) and the moduli are determined by the slope of the linear region. The load cell and LVDT used in this work are calibrated annually by the manufacturer and have shown no significant changes over several years. The LVDT was also checked against a machinist type dial indicator gauge between calibrations and no discrepancies were found.

Triaxial Experiments

Dependence on Position and Orientation in Cast. Samples of Standard Comp B obtained from the 105 mm split mold casts and from the smaller cardboard tube casts were studied in triaxial loading using the confined cylinder geometry illustrated in figure 2 and discussed above. The axial stress, σ_A, and the axial strain, ε_A, were measured and the radial stress, σ_R, was calculated as indicated above. A typical curve of σ_R versus σ_A at 35°C is given in figure 3 showing the linear nonyield region at low σ_A and the linear yield region at higher σ_A. Poisson's ratio was obtained from the slope in the nonyield range using equation 6 and the yield strength was obtained by the intercept method as illustrated in figure 3 and discussed in another section. A typical curve of σ_A versus ε_A at 35° C is given in figure 4 also showing the linear nonyield region at low σ_A, and the yield region at higher σ_A. The modulus E (Young's modulus) was obtained from the linear region using equation 7. Measurements were made to determine the yield strength, Y, the modulus, E, and Poisson's ratio, ν, as a function of position and orientation in the split mold cast at a strain rate of approximately 1.5 sec^{-1} and at a temperature of 35°C. Measurements were also made as a function of temperature between 20°C and 75°C at strain rates of approximately 6.7×10^{-4} sec^{-1} and 1.5 sec^{-1}. The latter measurements were made on samples obtained from cardboard tube casts.

Y, E, and ν are given in table 4 and figures 11 and 12 as a function of position and orientation at 35°C and at the high rate of loading. The uniaxial compressive strength and the modulus as obtained in uniaxial compression are also included in figures 11 and 12 for comparison purposes. The angle β, table 4, is the angle which the straight line for the yield region makes with the σ_A axis (see fig. 3). This angle is a measure of the effect of friction. An angle of 45° would indicate no friction while the amount of deviation from 45° is a measure of the amount of friction (see appendix).

The constants E and ν show no correlation with either position or orientation. The triaxial measurements of E are in excellant agreement with the value of $0.6 \pm 0.2 \times 10^6$ psi obtained from uniaxial compression measurements. The average value of ν is 0.34 ± 0.02.

There is no definitive dependence of Y on position or orientation. However, transverse samples cut from sections three and four show considerably more scatter in yield strength than samples cut from other sections and the average value is higher than the values from other sections. The average yield strength for all vertically cut samples is 6900 $\pm$ 400 psi. Thus, these results suggest but do not confirm that the yield strength may be somewhat higher for transverse cut samples and/or samples cut from the middle sections of the cast. The average yield strength for this cast for all samples measured is 7,100 psi while the average uniaxial compressive strength is 3,260 psi. Thus, the ratio of yield strength to compressive strength is approximately 2.2 at 35°C for a strain rate of 1.5 sec^{-1}.

Dependence on Temperature and Strain Rate. Samples obtained from the cardboard mold casts were investigated as a function of temperature between 20°C and 75°C. Two strain rates were used, a low strain rate of $6.7 \times 10^{-4} sec^{-1}$ to determine quasi static information for modeling cast cooling and thermal cycling and a higher strain rate of approximately 1.5 sec^{-1} to give information pertinent to modeling in the artillery launch time frame.

The low rate or quasi static results are summarized in table 5 and figures 13, 14, and 15. The general trend with increasing temperature is a decrease in Y and E and an increase in ν. While the decrease in Y with increasing temperature is quite marked (see fig. 13) the decrease in E is small for the temperature range considered. The increase in ν with temperature is also small (see fig. 15).

Clark and Schmitt (ref 4) report a decrease in E and a small increase in ν with increasing temperature as determined by quasi static uniaxial compression. The results given in table 3 also indicate that E decreases with increasing temperature for uniaxial compression. With increasing temperature, decreases in the yield strength and stiffness, E, and increases in lateral movement, and so ν are expected.

The higher rate data is summarized in table 6 and figures 16, 17, and 18. The results are similar to the results for low rate. With increasing temperature, Y decreases significantly, E decreases but there is considerable scatter in the data and ν increases slightly. While the data of Clark and Schmitt (ref 4) also suggest a decrease in Y with increasing temperature, the temperature range, number of measurements and scatter in the data are too great to make conclusions regarding this temperature dependence from their results. In figure 17 the values of E obtained from triaxial experiments using samples from the 105 mm split mold and values from uniaxial compression are also plotted. Within a rather large scatter in the data the values of E from the two sources are in agreement. The reason for the large scatter in the values of E is not understood at this time, but undoubtedly is dependent on sample perfection.

Clark and Schmitt (ref 4) determined E and ν as a function of temperature in quasi static uniaxial compression by using strain gauged samples, limiting stresses to values much less than the failure stress and making measurements on one sample at several temperatures. A waiting time was allowed between measurements at a given temperature to allow reversible residual strain recovery.

While there is also considerable scatter in their data, the results for any one sample clearly show a decrease of E with increasing temperature. An increase of ν with temperature was also found but the values at higher temperature (50°C) are larger than values reported here and values close to 0.5 are indicated.

A comparison of the data for quasi-static or low-rate conditions with that for the higher rate indicates, as already noted, the same general trend as a function of temperature for both rates. However, the results suggest that the yield strength at higher rate is somewhat greater than the yield strength at the low rate. This can be seen by a comparison of figures 13 and 16. Because of scatter in the data this conclusion is only tentative. It is clear that the uniaxial compressive strength is more rate dependent than the yield strength (see figs. 10, 13, and 16). Young's modulus, as determined from triaxial measurements, is also somewhat lower for the low rate than for the high rate (compare figs. 14 and 17). From the data of table 3, Young's modulus, as determined from uniaxial compression experiments, is also lower at the lower rate than at the higher rate. Again, however, the scatter in the data gives some uncertainty to this conclusion. While the values of Poisson's ratio at low rate are at all temperatures slightly lower than the values at the higher rate (see figs. 15 and 18), the differences are probably not significant. The results of Clark and Schmitt also indicate a larger E at a higher rate but here also the scatter in the data is too great for conclusions to be made. The scatter in their reported values of ν are much too great to determine a rate dependence.

Variations of Composition B

Uniaxial Experiments

The two lots of samples of nonstandard Comp B, i.e., Comp B I and Comp B II (see table 1), which were cast in the 105 mm split molds, were compressed at a strain rate of 1.5 sec^{-1} and at room temperature to investigate the effects of position and orientation on the compressive strength and the elastic modulus. Figures 19 and 20 show the results of these experiments. The ordinate is the compressive strength and the abscissa is the location along the axis of the 105 mm split mold from which the samples were taken. A T indicates that the cylindrical samples were cut with axis transverse or perpendicular to the shell (cast) axis while the V indicates vertical or parallel to the axis. Section 1 corresponds to the nose of the shell, the end at which the material was poured, and section 6 is the base of the shell (see fig. 7).

The compressive strength of samples taken from a cast of Comp B II which contained fine RDX, military grade TNT, and wax showed some dependence on position, while the strengths of samples taken from a cast of Comp B I which contained RDX, recrystallized TNT, and no wax, showed a much greater dependence on position. The compressive strengths of samples taken from the base were approximately 50% higher than for samples taken from the nose. From the available data and from the way samples were taken it was not possible to determine differences between samples cut vertical or transverse to the axis. However, other previous

work has shown differences not only between vertical and transverse samples, but also between samples taken from the top and bottom of a cast.[2] This investigation found that the transverse samples are stronger than the vertical samples. In addition, samples taken from the bottom of the cast were stronger than samples from the top of the cast.

The differences in compressive strengths between the two casts may be related to the differences in compositions and possibly cast quality. Coarse RDX may tend to settle out more rapidly while the cast is cooling, thus causing a gradient in the RDX concentration larger than in the fine RDX cast. The variation in strength with position can then be caused by concentration gradients of RDX. Since TNT is weaker than Comp B, it is reasonable to say that up to a limit, compressive strength should increase with RDX concentration. Also, it is more likely that imperfections in the cast, such as piping voids or air bubbles, would be toward the top of the cast. Orientational effects on compressive strength can be caused by anisotropic crystallite formation of the TNT. Also, military grade TNT has small concentrations of impurities such as mononitrotoluene (MNT), which are thought to act as plasticiers. A low level of MNT along with the absence of wax, would tend to make the cast more brittle and the compressive strength possibly higher, and would cause difficulties in casting, as mentioned previously.

It is also significant to note that the average compressive strengths of both Comp B I and Comp B II are higher than the compressive strengths of standard Comp B (see table 2). These results suggest that the finer RDX particles and/or the higher TNT purity and absence of wax both increase the compressive strength. The lack of positional dependence of the compressive strength for the standard Comp B suggests insignificant concentration gradients and a better quality cast. The latter was observed by x-ray radiography.

Triaxial Experiments

The yield strengths of Comp B I and Comp B II were measured using the triaxial loading technique described above. The yield strengths were found to be approximately 30% higher for both of these Comp B's than the values obtained using standard Comp B. However, the scatter in the data is also large, suggesting that there were differences in the samples. Additional experiments are necessary to resolve this matter.

---

[2] D. Georgevich, private communication.

TNT

Uniaxial Experiments

Experiments similar to those performed on Comp B were performed on TNT. These experiments were performed to determine the effects of adding RDX and wax to TNT to make Comp B. In addition, TNT is an important material by itself. Military grade TNT was cast in the 105 mm split mold and in cardboard tubes. Measurements were made as a function of position and orientation, and as a function of temperature and strain rate as for Comp B.

Samples were studied in uniaxial compression as a function of position and orientation and a typical stress/strain curve is given in figure 21. This curve is to be compared to figure 1 for Comp B. The modulus and σ_m are lower for TNT. σ_m and E are given as a function of position and orientation in table 7 and figures 22 and 23. From the results, it is concluded that there is no obvious dependence of σ_m or E on position or orientation for this cast of TNT within the limitations of the data.

The limited data as a function of temperature and rate are summarized in table 8 and figure 24. σ_m decreases as temperature is increased at both rates. There is also an increase of σ_m for all three temperatures as the rate is increased. Both the temperature and rate dependencies are the same as for Comp B. The low rate data is in agreement with the results of Costain and Motto (ref 3). While there is considerable scatter in the modulus E values, E does decrease as temperature is increased and does increase as rate is increased as shown in table 8. Although the E values, as determined in this work, are smaller than the values reported by Clark and Schmitt (ref 4) the temperature dependence is similar.

Triaxial Experiments

Samples of TNT were studied in triaxial compression as a function of position and orientation as were samples of Comp B. Typical σ_A versus σ_R and σ_A versus ε_A curves are given in figures 25 and 26. The results are summarized in table 9, and figures 22 and 23. These data indicate little or no dependence of Y, E, or ν on position or orientation within the limits of scatter of results. In addition, the moduli as obtained from uniaxial measurements, are in agreement with the values obtained from triaxial measurements. The σ_A versus ε_A curve as given in figure 26, indicates a region of plastic flow as evidenced by the tendency to plateau after the linear elastic region. This "plastic flow" region may be due to the collapse of voids during compression. Visual examination of the TNT samples before compression indicates considerable porosity. Comp B gave similar σ_A versus ε_A curves at high temperature.

From the data, it can be concluded that the compressive and yield strengths and the moduli for TNT are smaller than similar values for Comp B. The values of Poisson's ratio for TNT are the same or slightly larger than values obtained for Comp B. Thus the addition of 60% RDX (and 1% wax) to TNT to make

Comp B has the effect of stiffening the material since the moduli of Comp B are greater than the moduli of TNT. In addition, the uniaxial compressive strength and the triaxial yield strength are increased by this addition of RDX, thus indicating that RDX makes the material stronger.

The ratio of the triaxial yield strength to the uniaxial compressive strength for TNT is approximately 1.7. This ratio for Comp B was found to be approximately 2.2. Within the precision of the data this ratio is not strongly affected by the addition of 60% RDX. The yield strengths reported by Clark and Schmitt (refs 2 and 5) are larger than the values reported here as is the case for Comp B. This difference suggests a systematic error. The moduli reported by Clark and Schmitt are too scattered to be compared with the results reported here. The temperature and rate dependencies, as given by table 8 and figure 24, exhibit the same trends as given above for Comp B and are most probably due to the same causes.

DISCUSSION

Position and Orientation Dependence

For one cast each (from split mold) the values of compressive strength σ_m and Young's modulus for Comp B and TNT were found to be, within the scatter of the data, independent of position and orientation of the sample in the cast before cutting. These results indicate homogeneous casts. The results for Comp B then suggest that RDX has not settled to give a significant gradient of RDX concentration versus position.

The dependence of σ_m on position for Comp B I and Comp B II indicates the type of results obtained from a nonuniform cast of explosive. As indicated above, the dependence of σ_m on position may be due to gradients of RDX concentration.

Temperature and Rate Dependence

The compressive strength, σ_m, the yield strength, Y, and Young's modulus, E, were found to increase as temperature decreased although there is considerable scatter in the data particularly in the modulus results. Poisson's ratio, ν, was found to increase slightly with increasing temperature as the temperature approached the melting point. In addition, σ_m and Y were found to be higher at the high strain rate ($\dot{\epsilon} = 1.5\ \text{sec}^{-1}$) than the values at low strain rate ($\dot{\epsilon} = 6.7 \times 10^{-4}\ \text{sec}^{-1}$).

As temperature increased, the modulus decreased as noted. Thus, the decrease of σ_m with increasing temperature may at least in part be attributed to a decrease in the critical stress for crack movement through the dependence on modulus (ref 5). The scatter in the modulus data is too great to give the

functional dependence of modulus on temperature. The surface energy of a crack may also decrease with increasing temperature and so account for some of the decrease of σ_m. The temperature dependence of the yield strength may be due to the unpinning of dislocations or to other thermal barriers to dislocation motion and generation (ref 6). The decrease of the modulus with increasing temperature may be due to a softening of the lattice with increasing temperature. The temperature dependence of Poisson's ratio is due to the same factors.

The increase of σ_m and Y with increasing rate are typical of viscoelastic materials (ref 7). While Comp B is not a polymeric material, relaxation processes may give the same results. The dependence of these quantities on temperature is also the same as for viscoelastic materials. Additional work is required to give the temperature and rate dependencies more precisely.

The limited measurements on TNT samples indicate that TNT has the same dependencies on temperature and rate as Comp B. The compressive strength, the yield strength, and the modulus are all smaller for TNT than for Comp B, thus indicating that 60% RDX in TNT strengthens and stiffens the material. Finally, it should be noted that crack propagation may be hindered at RDX particles and thus increase σ_m for Comp B relative to TNT.

Friction

Friction can influence the results of these experiments. For example, in uniaxial compression there are frictional forces between the sample ends and the platens of the apparatus. Thus, the sample ends are not in simple uniaxial compression. It is assumed in this work that these end effects are not important and that the stresses become effectively uniaxial compressive stresses at short distance from the ends and that the samples fail in compression.

In triaxial compression the primary influence of friction will be because of the interaction between the sample side wall and the inner surfaces of the confining cylinder. While graphite was applied to these surfaces the effect of friction could only be minimized. The effects of friction are considered in the appendix. The results are that the yield strength as determined by the intercept method is independent of friction, but the slopes of the σ_R versus σ_A curve in the elastic and the yield regions are decreased by friction. The slopes of the curves in the yield region are found to be less than one, indicating that friction is present. However, the values of ν and E were calculated neglecting friction. The corrections for friction are small and are neglected because of the large scatter in the values of ν and especially of E.

REFERENCES

1. S. Serata, "Transition from Elastic to Plastic State of Rocks Under Triaxial Compression," Bulletin of Mineral Industries Experiment Station, Proceedings of the Fourth Symposium of Rock Mechanics, Number 76, 1961, p 73, Pennsylvania State College.

2. N. Clark and F. Schmitt, "Techniques for the Determination of the Yield Strength of Composition B," Engineering Sciences Division Information Report No. 558, Picatinny Arsenal, Dover, NJ, 1972.

3. T. Costain and R. Motto, "The Sensitivity, Performance and Material Properties of Some High Explosive Formulations," Technical Report 4587, Picatinny Arsenal, Dover, NJ, September 1973.

4. N. Clarke and R. Schmitt, Unpublished Report.

5. H. Liebowitz (Ed.), "Fracture," Academic Press, vol VII, 1972, p 168.

6. H. Liebowitz (Ed.), "Fracture," Academic Press, vol VII, 1972, p 88.

7. L.E. Nielson, Mechanical Properties of Polymer and Composites, Marcel Dekker, New York, p 9, vol I, 1974.

Table 1. Composition of Comp B I and Comp B II

	Comp B I		Comp B II
RDX	60%	Grade A (course)	59.4% Grade G (Fine)
TNT	40%	Recrystalized Military Grade (Purified)	39.6% Military Grade
Wax		None	1.0% Petrolite (ES-670)
HMX	7.4%	(of RDX)	9.3% (of RDX)

RDX PARTICLE SIZE DISTRIBUTION

Sieve number	Grade A % passage	Grade G % passage
20	100%	100%
50	93.6	97.0
100	34.4	66.8
200	11.0	56.5
325	0	
TNT	Recrystallized	Military Grade
TNT Melting Point	82.5°C	82.5°C

Table 2. Summary of Comp B uniaxial compression data versus position and orientation - high strain rate

Sample	ρ (g/cm^3)	Temperature (°C)	σ_m (psi)	ε_m %	E x 10^6 (psi)
2V	1.694	23	3050	0.54	0.63
4T	1.695	23	3260	0.65	0.59
5V	1.693	23	3400	0.78	0.57
6V	1.691	23	3200	0.63	0.60

Table 3. Summary of uniaxial Comp B compression data versus temperature and strain rate

Sample	ρ (g/cm³)	Temperature (°C)	σm (psi)	εm (%)	E x10⁶ (psi)	$\dot{\varepsilon}$ sec^{-1}
C-16		23	1680	0.49	0.36	6.67×10^{-4}
C-20		40	1330	0.41	0.37	6.67×10^{-4}
C-9		40	1330	0.41	0.36	6.67×10^{-4}
C-14		60	880	0.40	0.26	6.67×10^{-4}
A-13		60	1140			6.67×10^{-4}
A-11		60	820	0.31	0.26	6.67×10^{-4}
C-17	1.682	23	2970	0.53	0.62	1.43
C-19	1.680	40	2050	0.53	0.43	1.43
C-15	1.685	60	2140	0.48	0.48	1.43
A-14		60	1840	0.35		1.43

Table 4. Summary of Comp B triaxial compression data versus position and orientation

T = 35°C, and High Strain Rate

Sample	ρ (g/cm³)	Y (psi)	E x 10⁶ (psi)	ν	β (degrees)
1-T	1.689	7100	0.51	0.34	40.0
2-V	1.692	6300	0.63	0.35	40.7
2-V	1.698	6800	0.67	0.34	39.1
2-V	1.694	7400	0.55	0.36	42.4
3-T	1.695	7000	0.64	0.35	42.9
3-T	1.697	9900	0.61	0.35	43.0
4-T	1.697	4000	0.56	0.37	36.4
4-T	1.697	8600	0.65	0.30	41.9
5-V	1.701	7000	0.66	0.34	40.1
6-V	1.697	7000	0.62	0.33	39.5
6-V	1.691	7100	0.47	0.35	39.4

Table 5. Summary of Comp B triaxial compression data versus temperature - low strain rate

Sample	Temperature (°C)	Y (psi)	E x 10^6 (psi)	ν	β (degrees)
9-2	20	6100	0.46	0.30	41.5
9-1	25	6100	-	0.29	40.6
5-2	30	5300	0.36	0.33	42.4
2-2	36	6700	0.70	0.32	42.8
2-3	36	4800	0.63	0.32	42.6
25-1	45	4700	0.40	0.34	41.6
25-3	45	5400	0.45	0.33	42.2
20-1	50	4400	0.38	0.33	41.2
14-1	50	4600	0.35	0.33	41.5
20-3	60	4600	0.39	0.34	43.2
16-1	70	2600	0.30	0.36	43.2
24-1	70	3100	0.34	0.35	43.2

Table 6. Summary of Comp B triaxial compression data versus temperature - high strain rate

Sample	Temperature (°C)	Y (psi)	E x 10^6 (psi)	ν	β (degrees)
A-16	22	8200	0.69	0.34	43.1
4-1	30	6900	0.55	0.37	41.0
27-3	30	6900	-	0.35	42.2
7-1	30	7900	0.58	0.30	40.2
9-3	30	7200	(.69	0.33	40.0
8-2	30	5800	-	-	41.1
2-1	38	7400	0.80	0.34	42.4
A-15	40	6500	0.53	0.32	40.6
A-12	40	5900	0.74	0.32	41.4
2-2	43	6300	0.63	0.35	40.7
14-3	45	6500	0.48	0.37	42.2
B-15	50	5000	0.61	0.35	41.1
21-1	50	6200	-	0.35	41.11
18-3	55	5200	0.49	0.38	42.6
B-14	60	4500	0.63	0.35	40.9
B-11	60	3700	0.58	0.33	40.3
B-1	60	4400	0.65	0.34	40.7
19-3	70	3000	0.54	0.35	40.4
28-3	70	4000	0.52	0.36	41.9
29-1	70	3600	0.57	0.35	39.8
12-1	70	4200	0.50	0.39	43.3
12-3	70	3800	0.40	0.40	43.2
C-18	75	2200	0.40	0.36	40.6
28-1	75	3000	0.50	0.37	42.6

Table 7. Summary of TNT uniaxial compression data versus position and orientation - high strain rate

Sample	σ_m (psi)	ε_m %	$E \times 10^6$ (psi)
1T	1710	0.68	0.35
2V	1940	0.49	0.56
3T	1860	0.57	0.42
4T	770	0.30	0.42
5V	1640	0.58	0.43
6V	2080	0.57	0.49

Table 8. Summary of TNT uniaxial compression data versus temperature and strain rate

Sample	Temperature (°C)	σ_m (psi)	ε_m %	$E \times 10^6$ (psi)	$\dot{\varepsilon}$ (sec^{-1})
14	23	2480	0.56	0.46	1.5
16	42	940	0.58	0.16	1.5
7	40	1760	0.50	0.46	1.5
10	60	1160	0.54	0.23	1.5
11	23	960	0.45	0.25	6.7×10^{-4}
18	40	500	0.50	0.13	6.7×10^{-4}
6	40	740	0.38	0.18	6.7×10^{-4}
9	60	500	0 41	0.14	6.7×10^{-4}
17	60	500	-	-	6.6×10^{-4}

Table 9. Summary of TNT triaxial compression data versus position and orientation - high strain rate

Sample	Temperature (°C)	Y (psi)	E x 10^6 (psi)	ν	β (degrees)
1-T	35	3800	0.51	0.35	41.5
2-V	35	3300	0.40	0.39	39.5
2-V	45	3300	0.32	0.38	41.4
3-T	35	3100	0.51	0.36	39.8
4-T	45	2800	0.36	0.39	40.3
5-V	35	3100	0.40	0.36	41.2
6-V	21	3200	0.50	0.35	38.4
6-V	35	3200	0.37	0.38	41.0

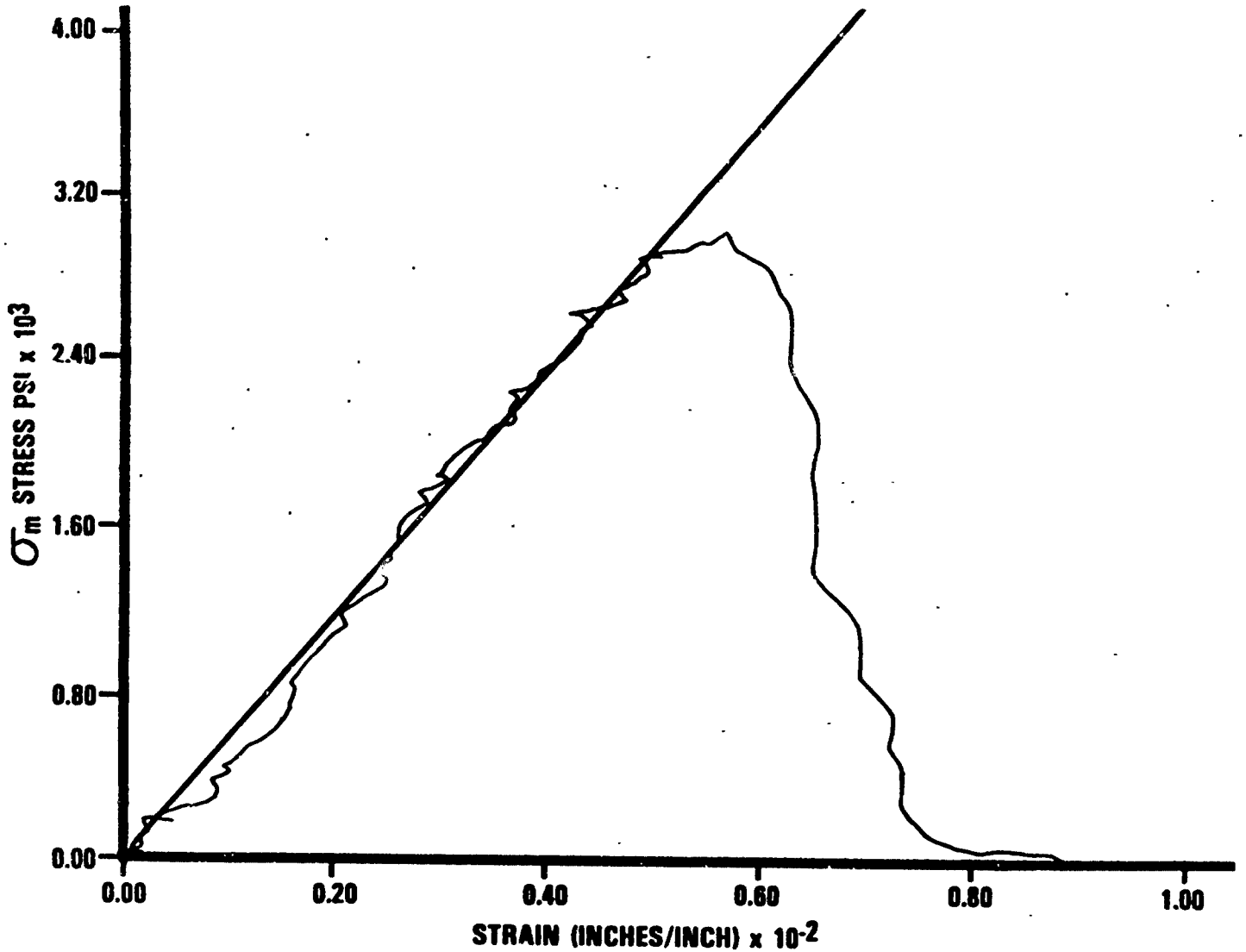

Figure 1. Typical stress, σ, versus strain, ε, curve for Comp B showing the determination of the modulus E. E is taken as the slope of the straight line part of the stress/strain curve

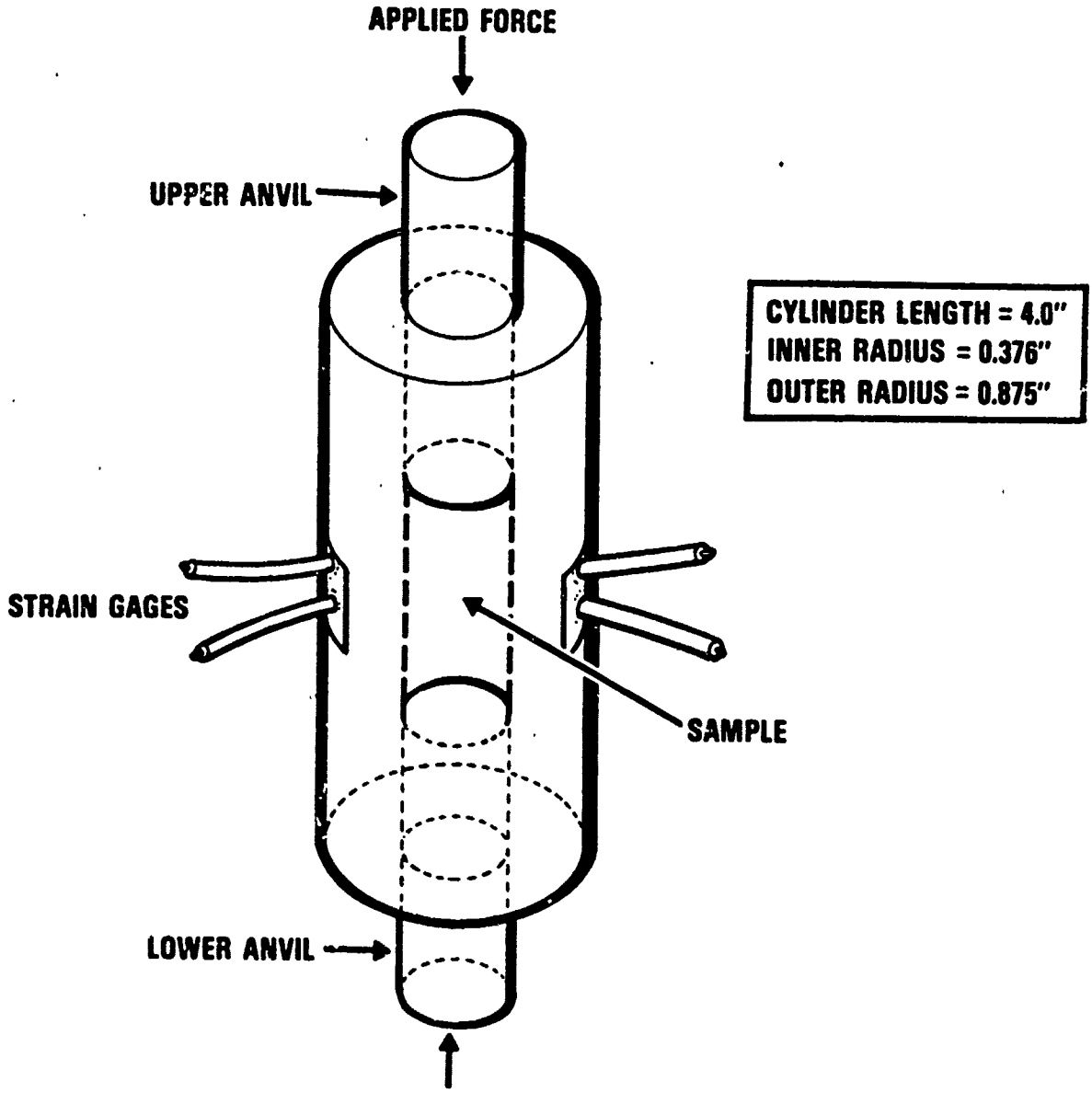

Figure 2. Confined cylinder triaxial experimental set up

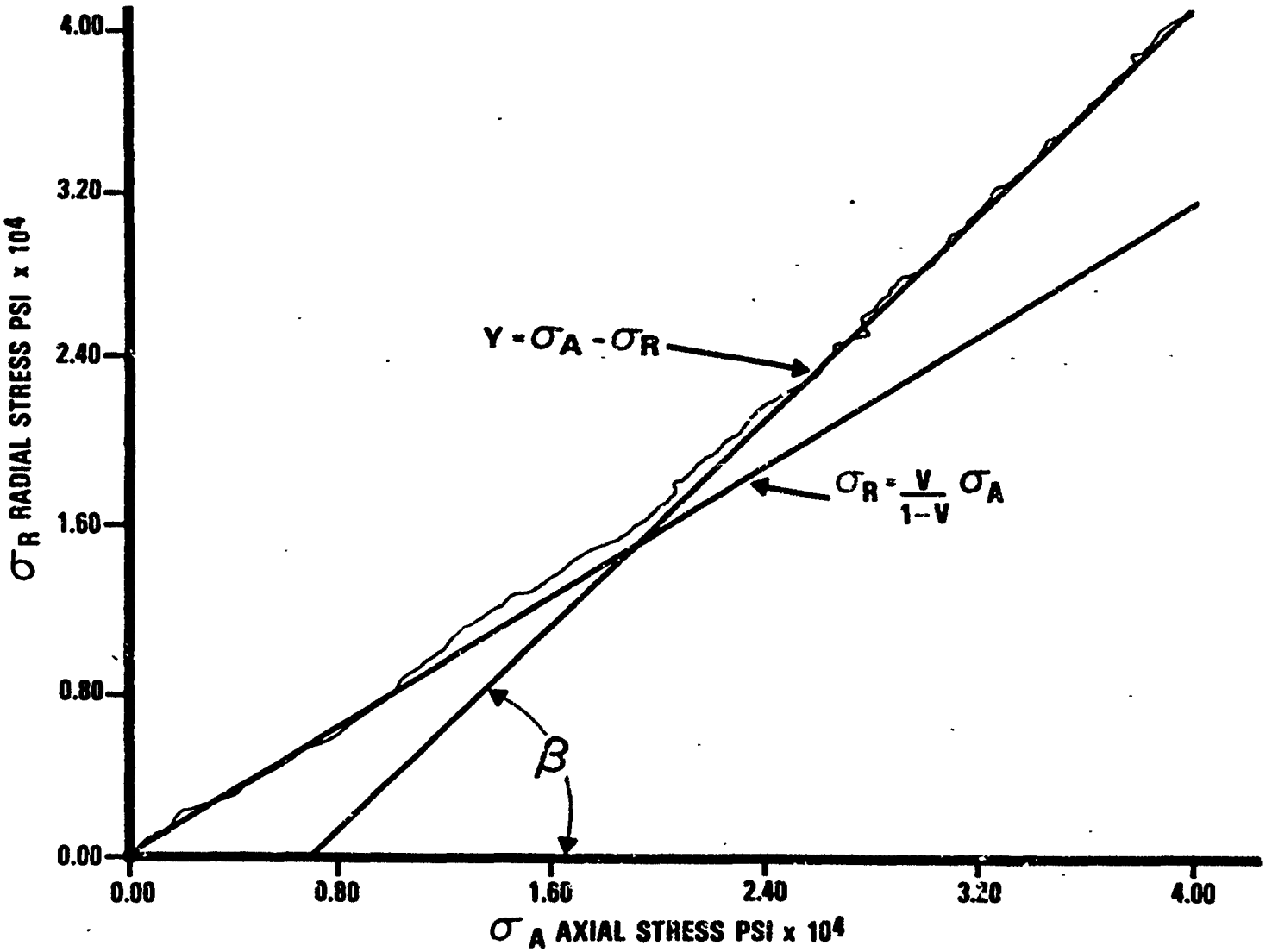

Figure 3. Typical radial, σ_R, versus axial stress, σ_A, curve for Comp B for confined cylinder geometry showing the linear elastic and the linear plastic ranges

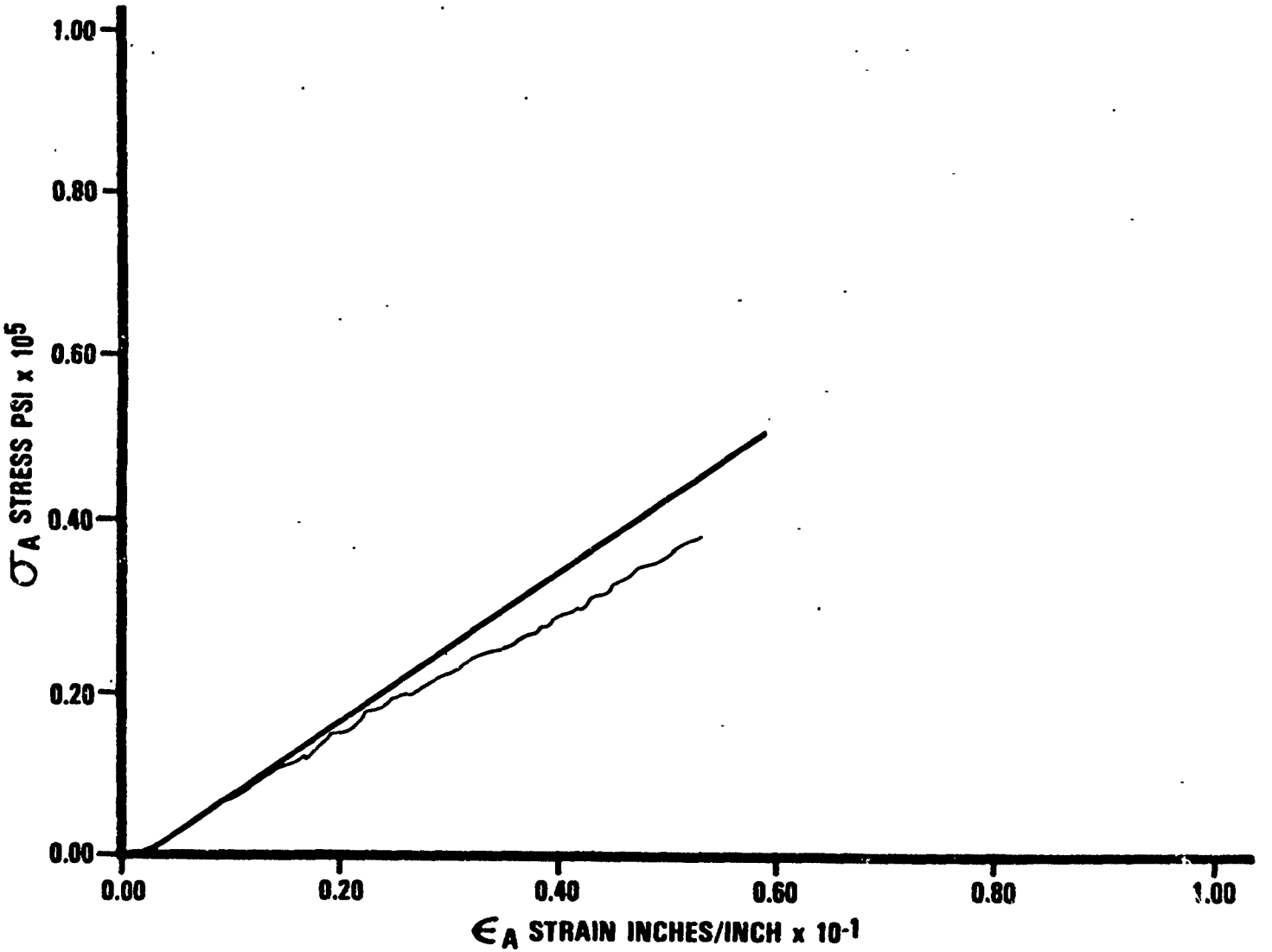

Figure 4. Typical axial stress, σ_A, versus axial strain, ε_A, for Comp B for the confined cylinder geometry

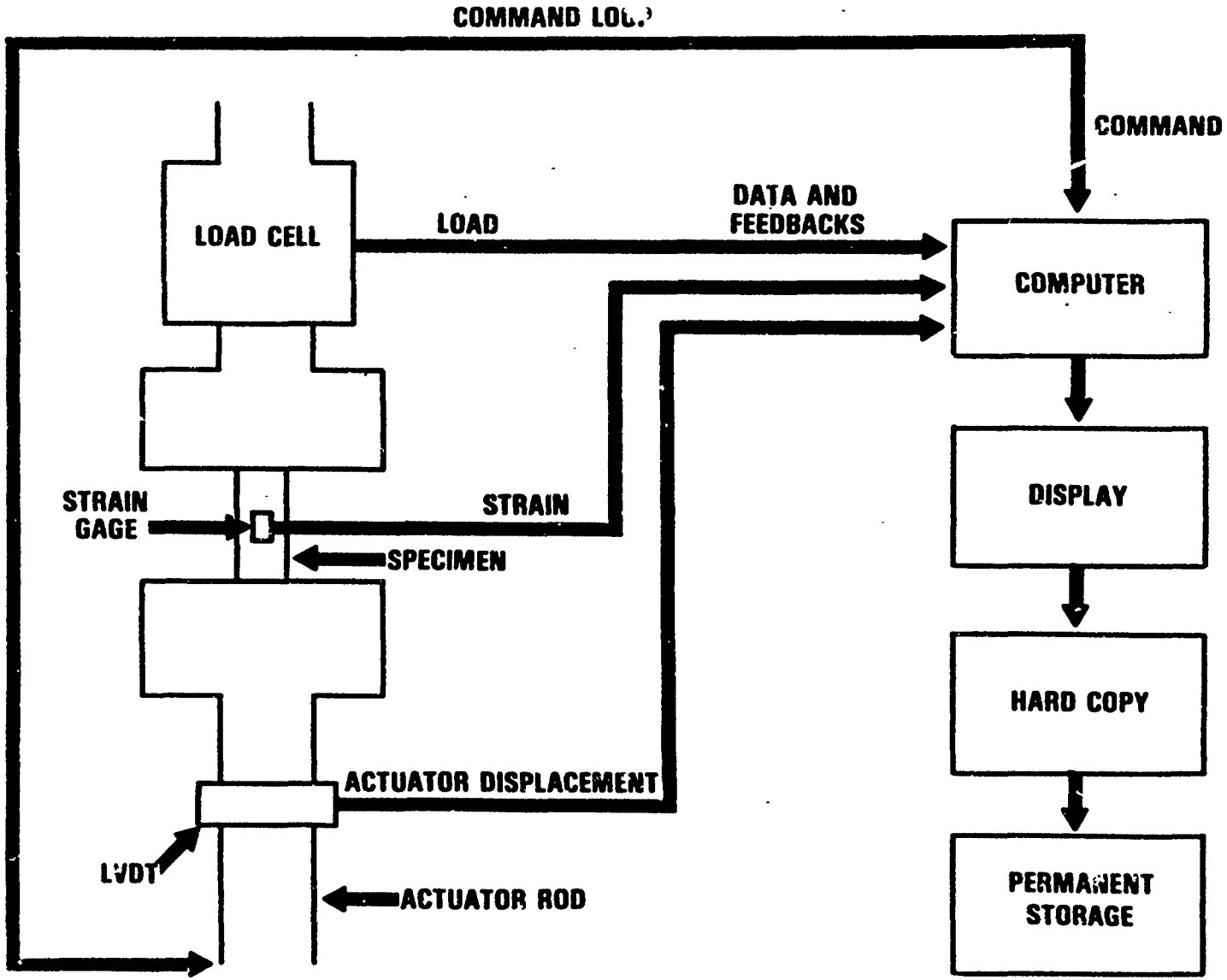

Figure 5. Block diagram of servo-hydraulic loading system and electronics

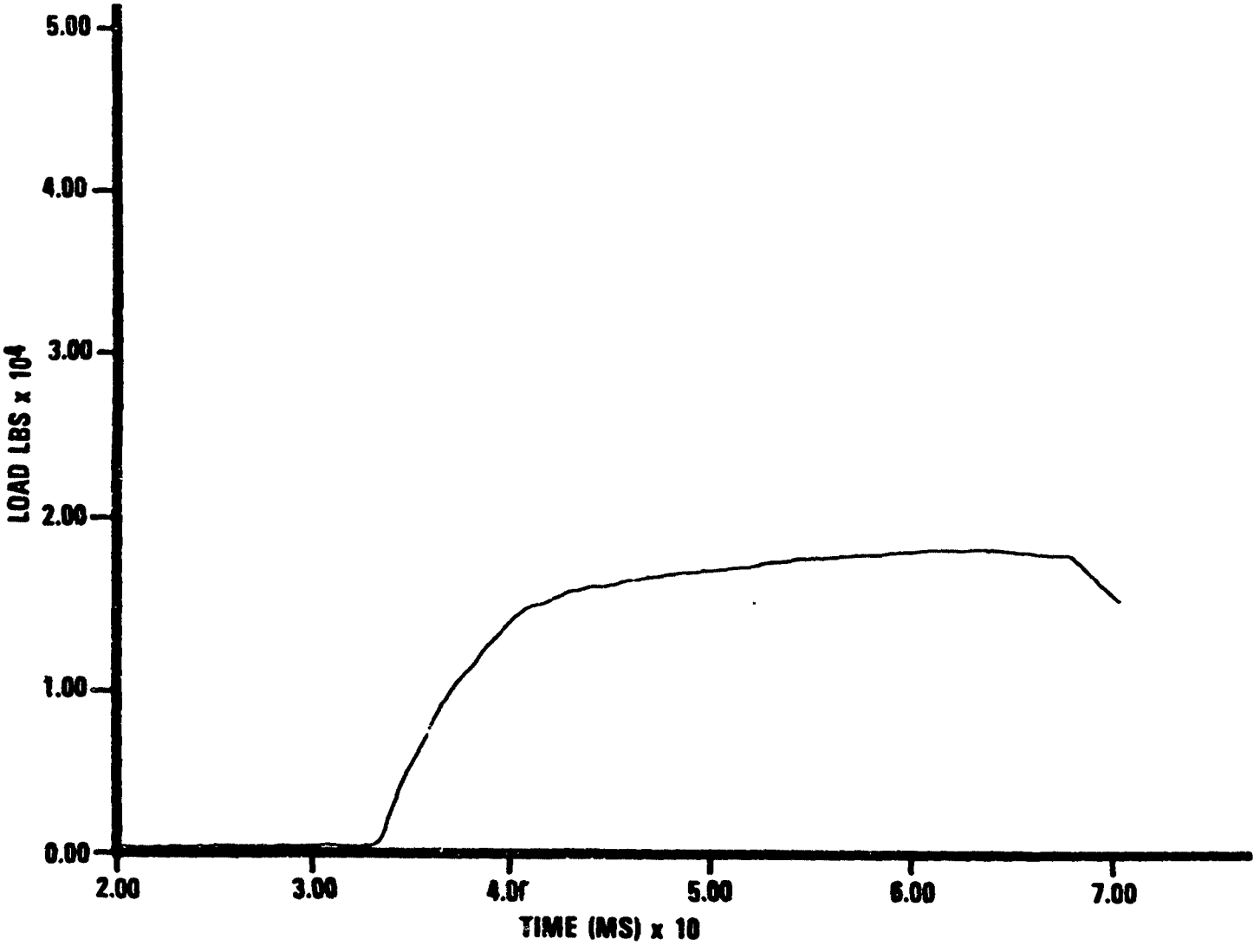

Figure 6. Typical "fast" axial load versus time curve for the confined cylinder test

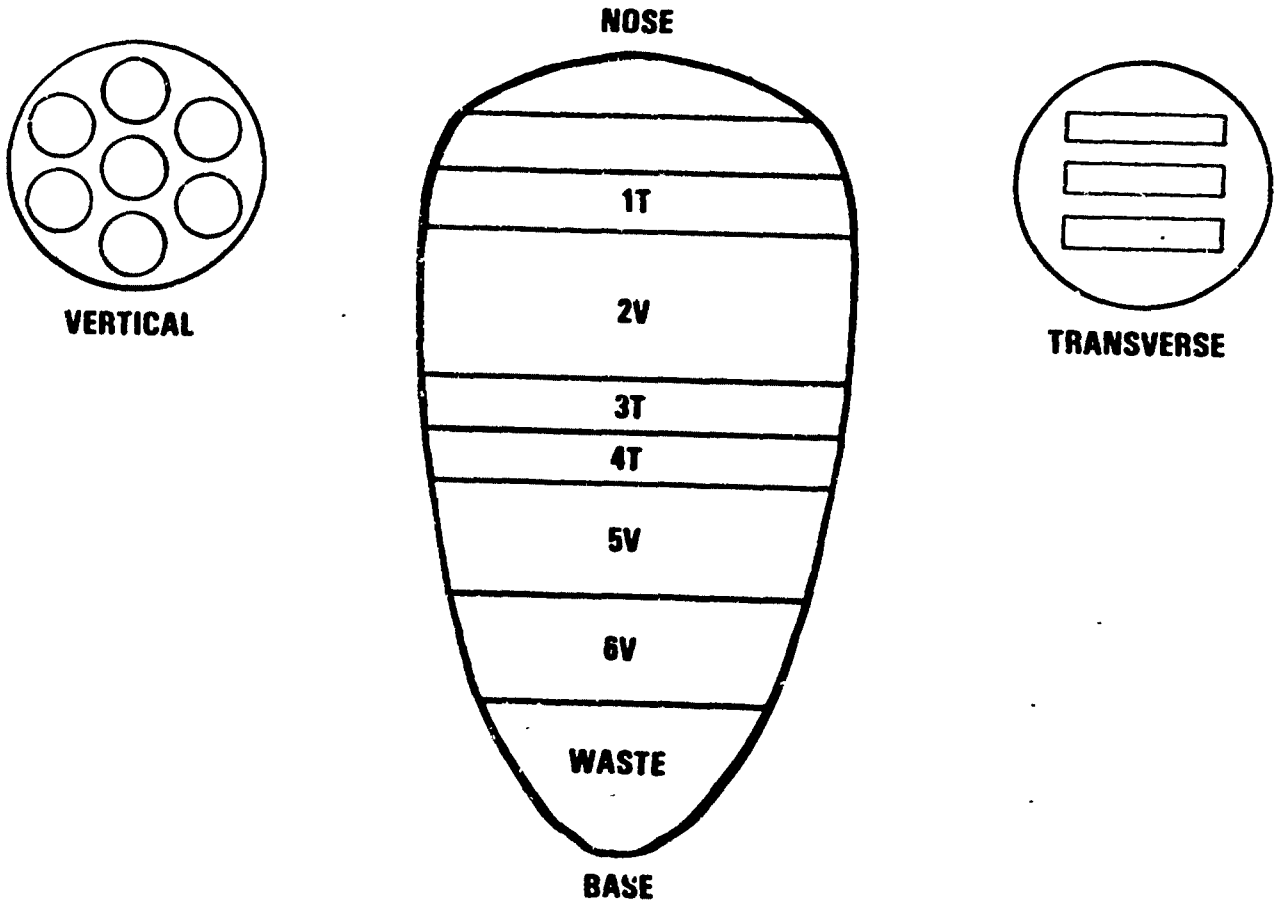

Figure 7. Diagram of a cast of Comp B obtained from the 105 mm split mold showing the transverse (V) and horizontal (H) sections and the way each type of section was cut into samples

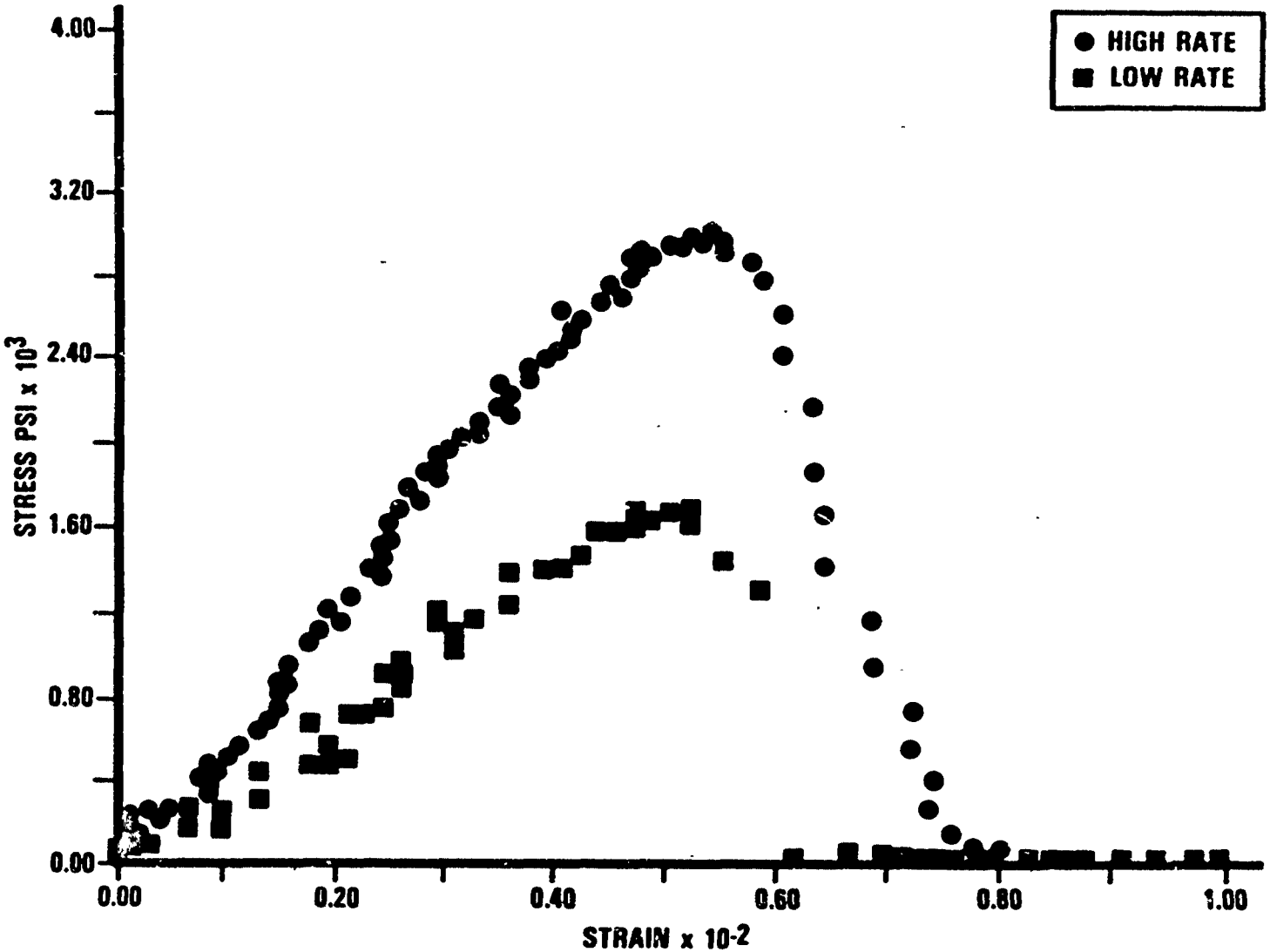

Figure 8. Typical uniaxial stress versus strain curves at 23°C and low and high strain rate

Figure 9. Typical Comp B samples after uniaxial loading to failure

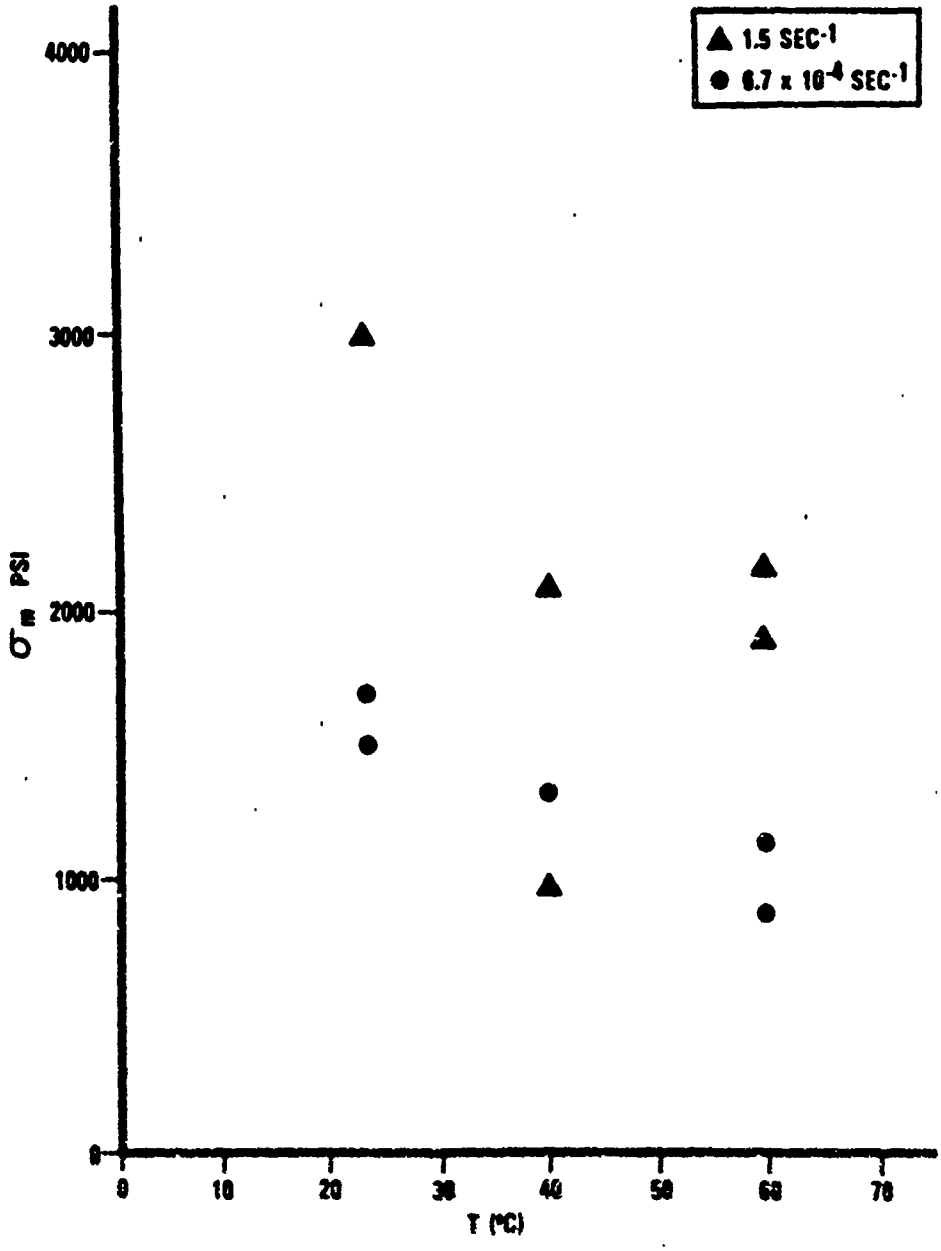

Figure 10. The compressive strength, σ_m, versus temperature for Comp B for low and high strain rates

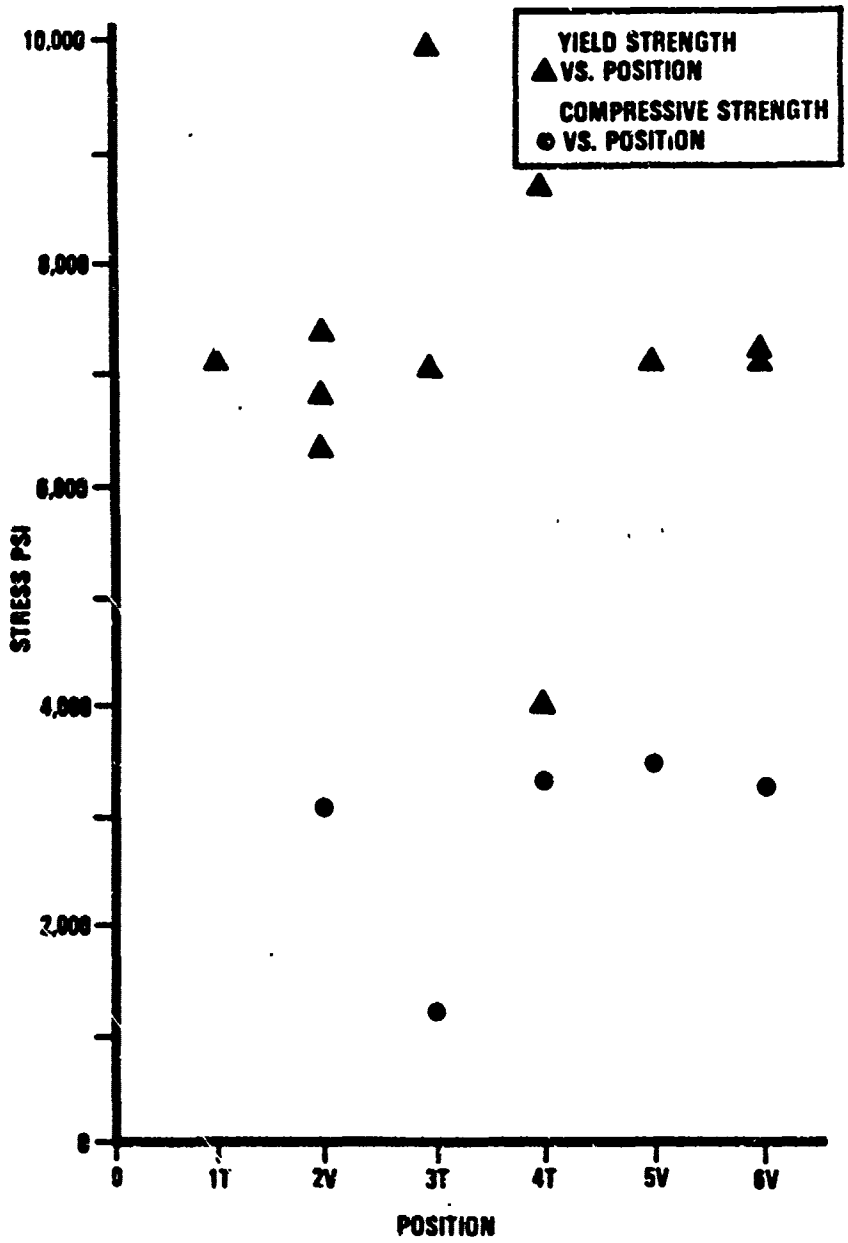

Figure 11. Uniaxial compressive strength, σ_m, and triaxial yield strength, Y, versus sample position and orientation in cast

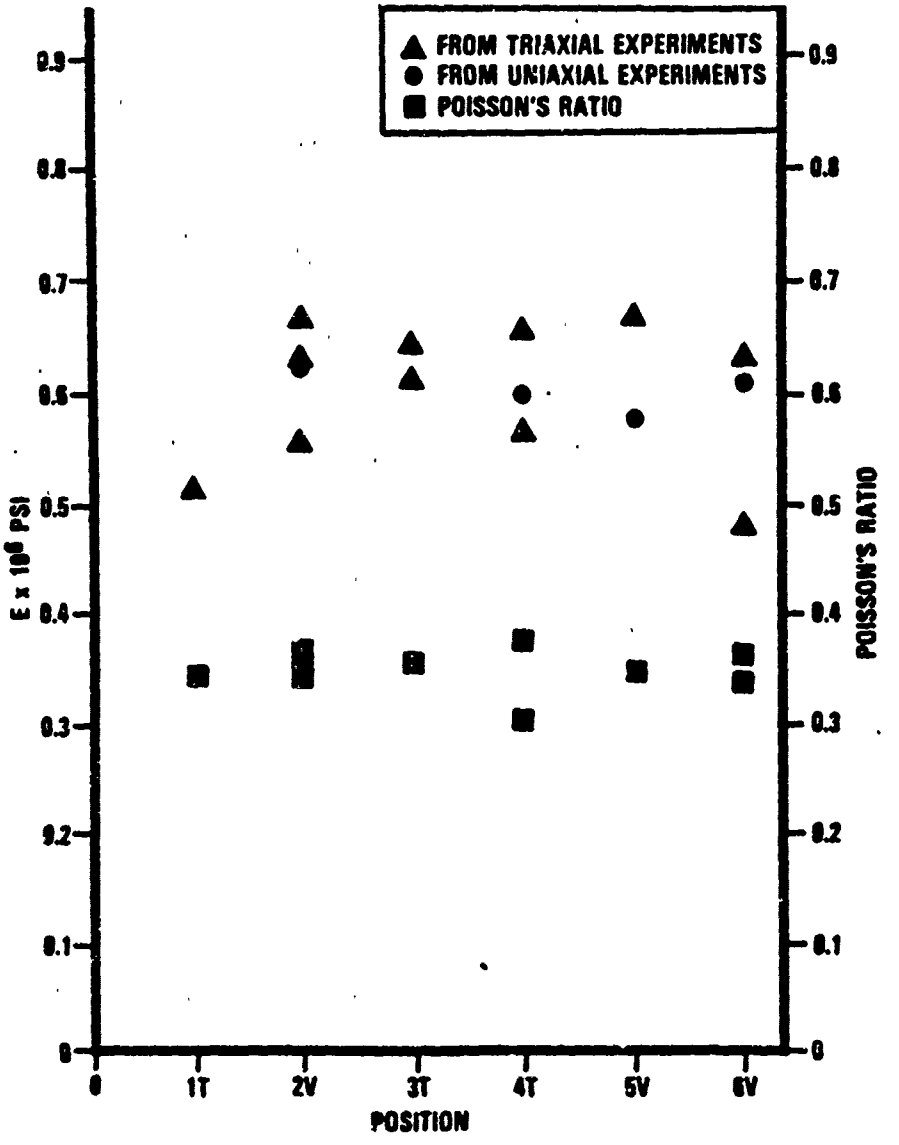

Figure 12. Young's modulus versus sample position and orientation in cast from uniaxial and triaxial loading. Poisson's ratio versus sample position and orientation from triaxial loading

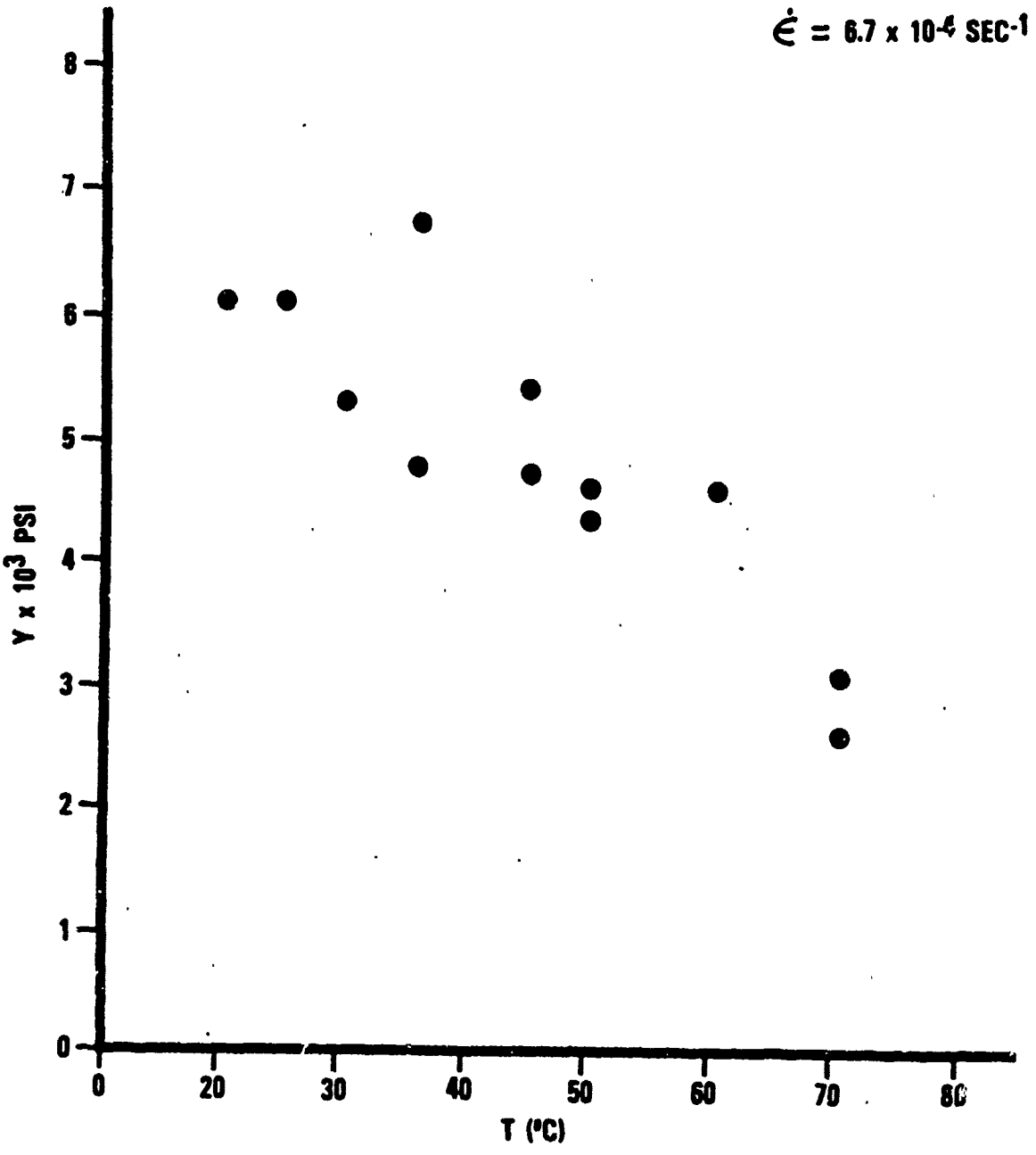

Figure 13. Yield strength, Y, versus temperature for Comp B - low strain rate

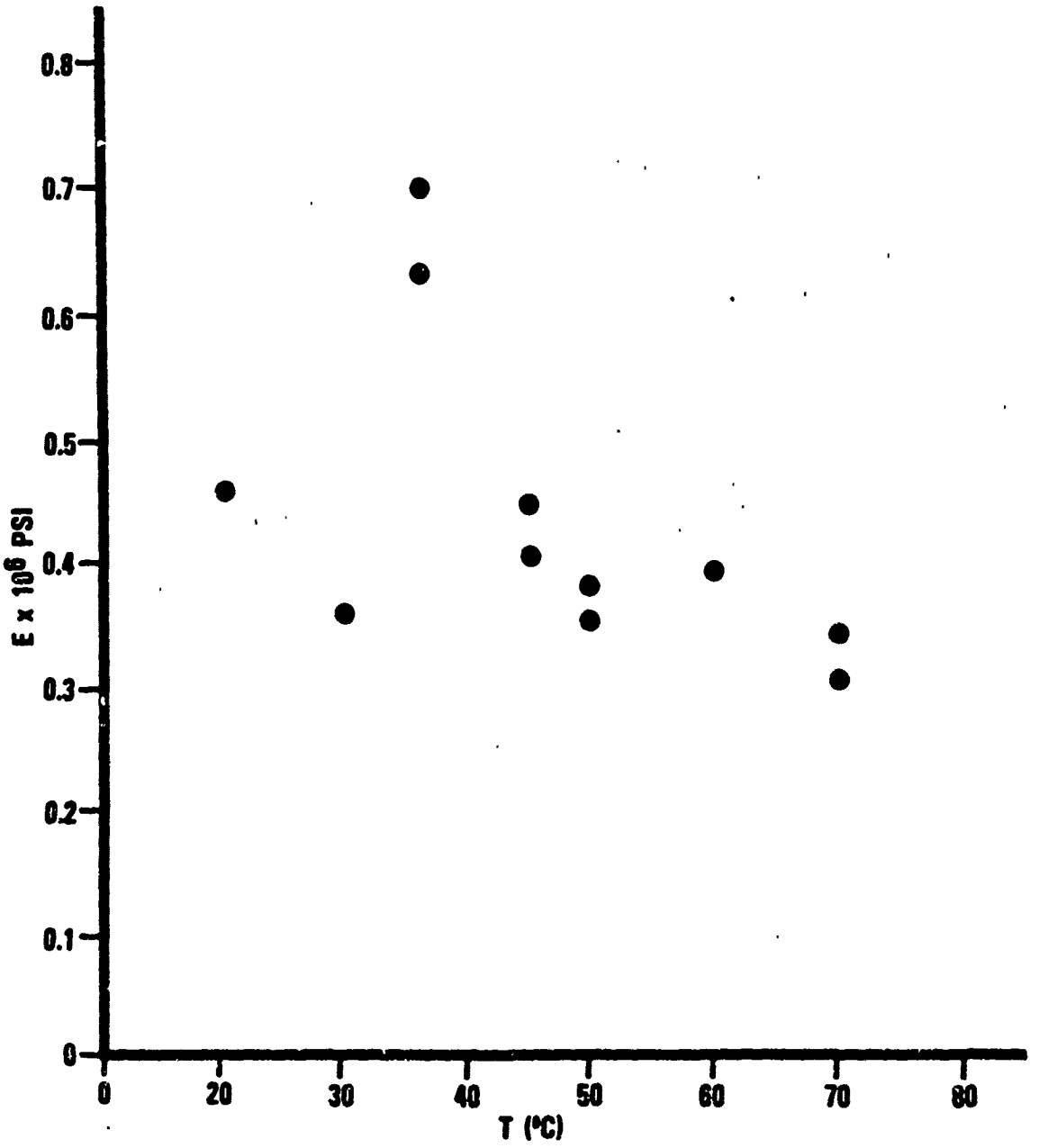

Figure 14. Young's modulus, E, versus temperature for Comp B - low strain rate

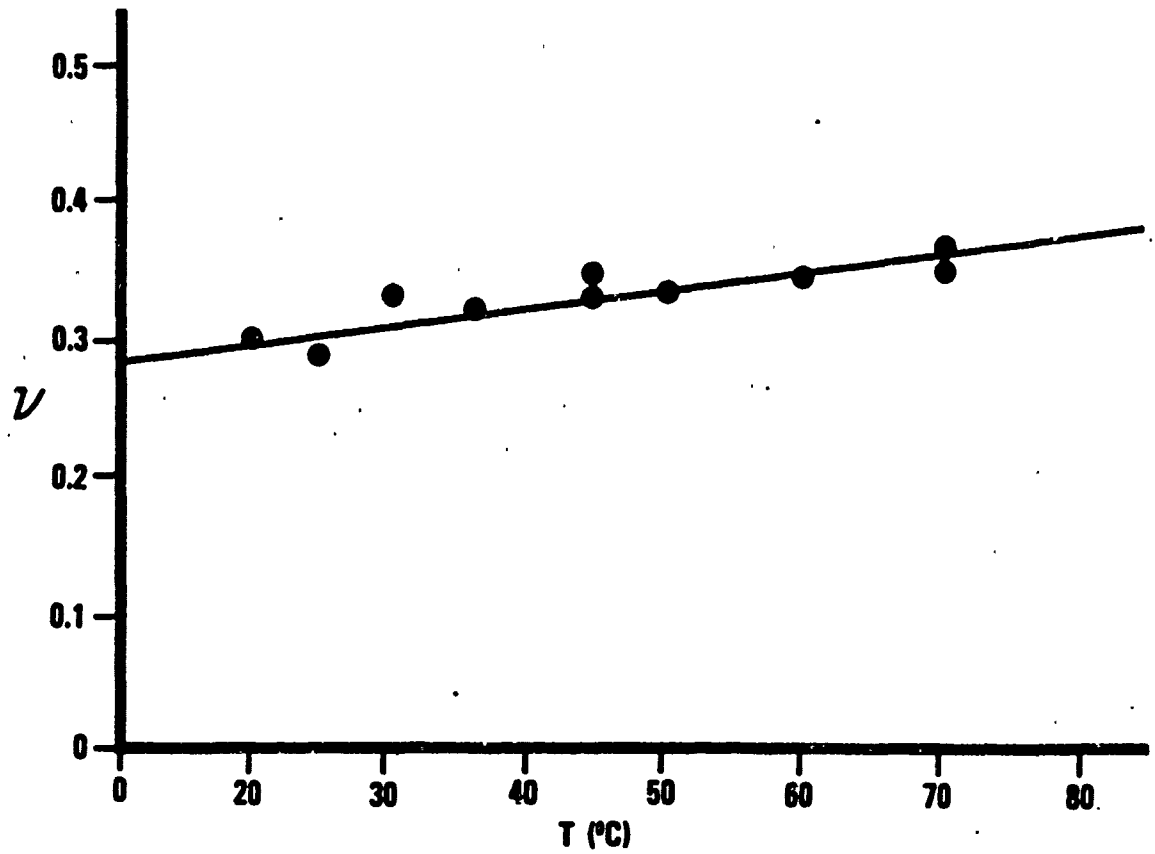

Figure 15. Poisson's ratio, ν, versus temperature for Comp B - low strain rate

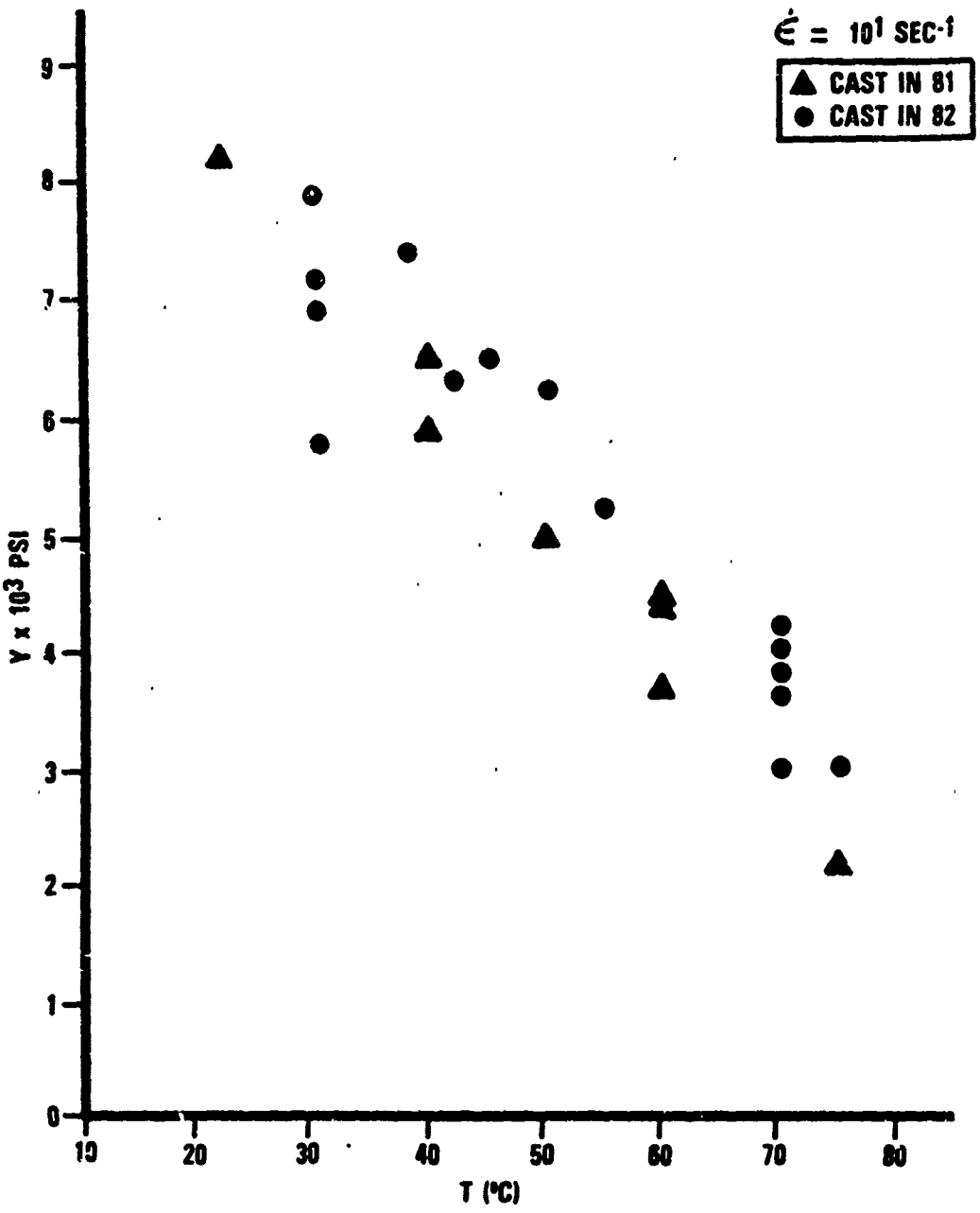

Figure 16. Yield strength, Y, versus temperature for Comp B - high strain rate

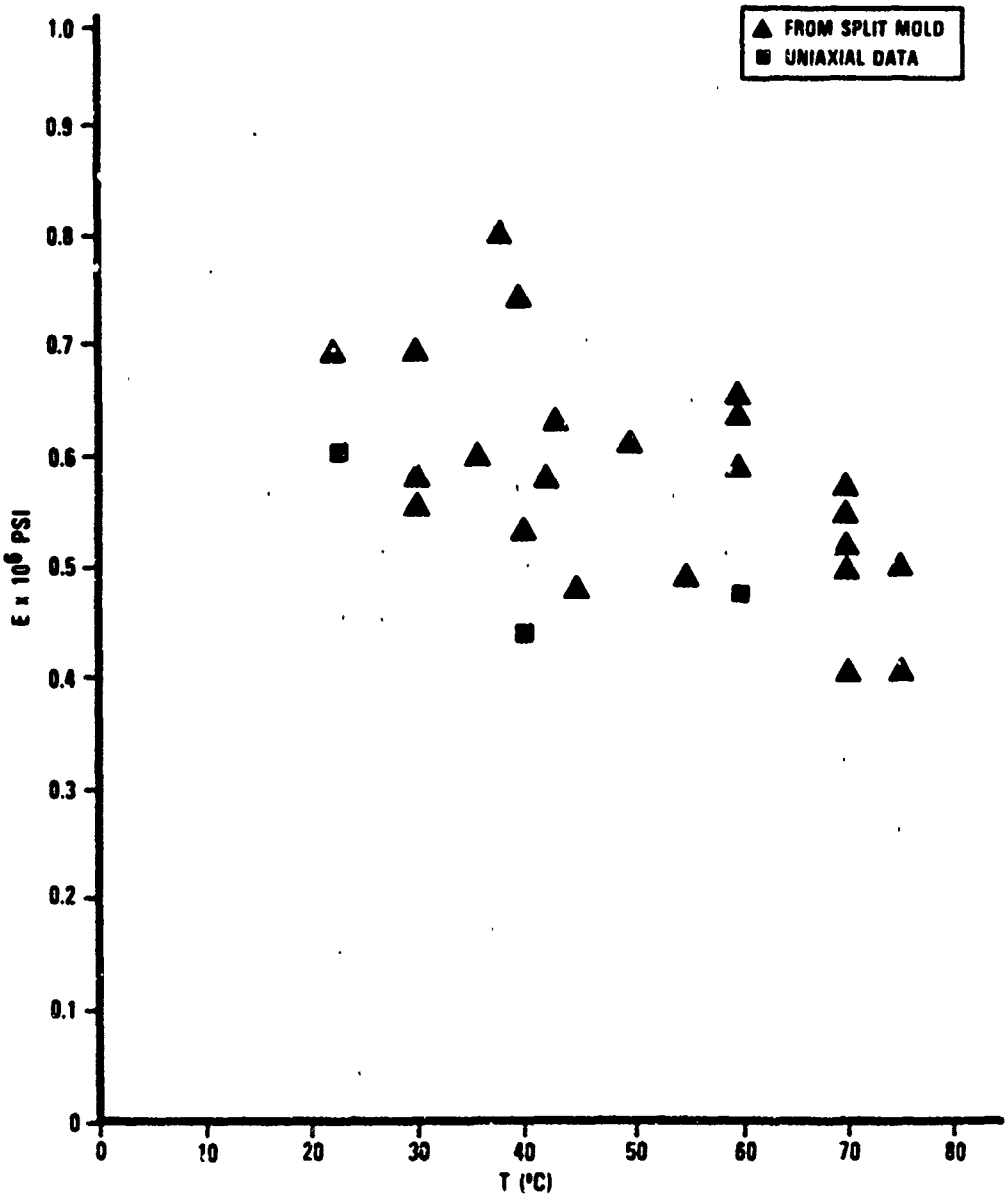

Figure 17. Young's modulus, E, versus temperature for Comp B - high strain rate

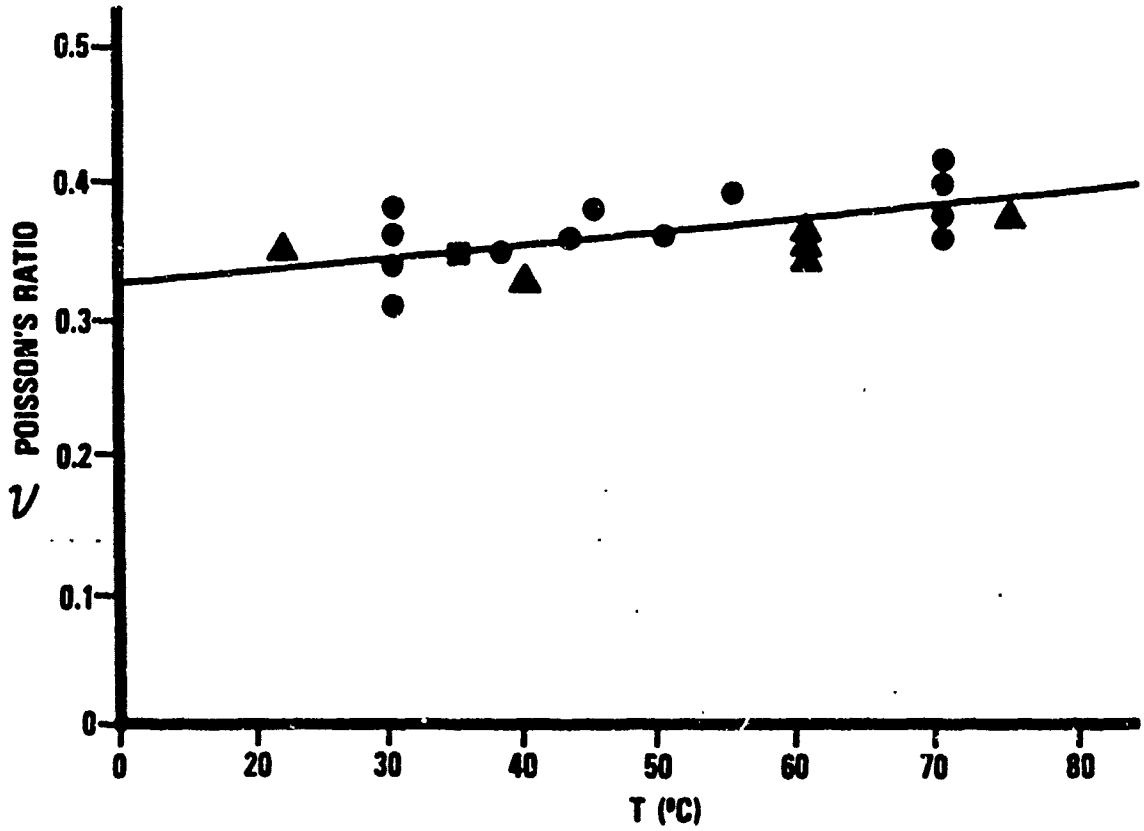

Figure 18. Poisson's ratio, ν, versus temperature for Comp B - high strain rate

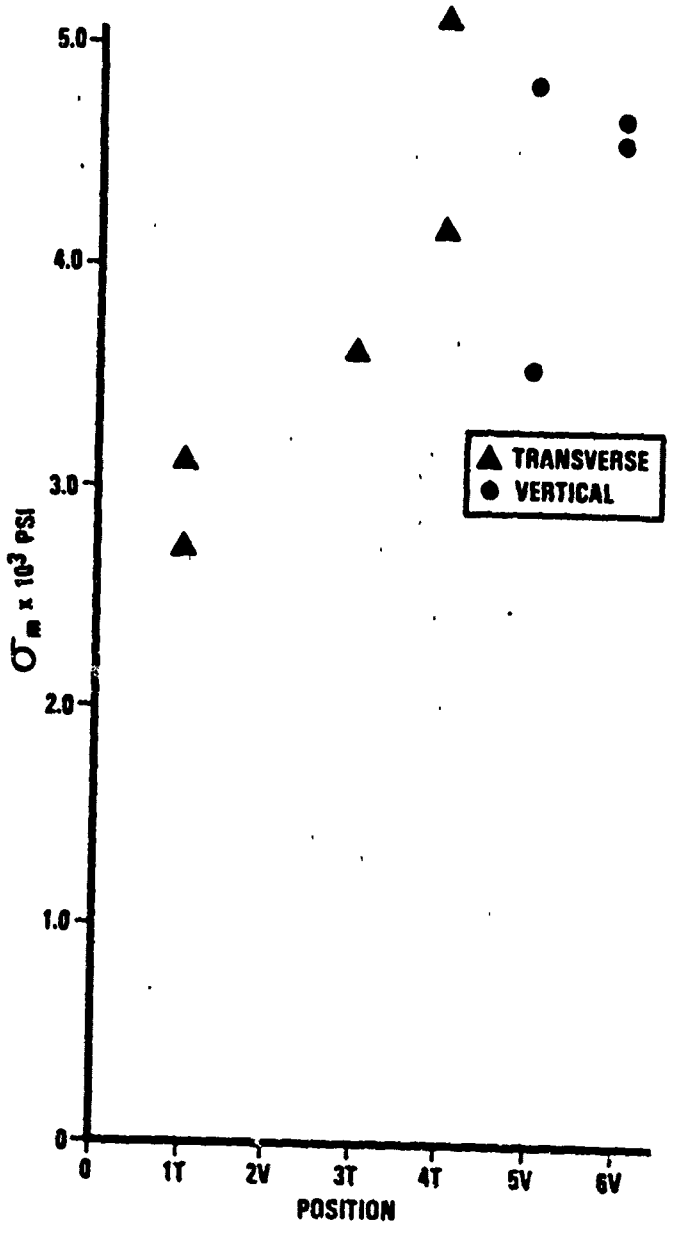

Figure 19. Compressive st ... , versus position and orientation of sample in cast ... B I

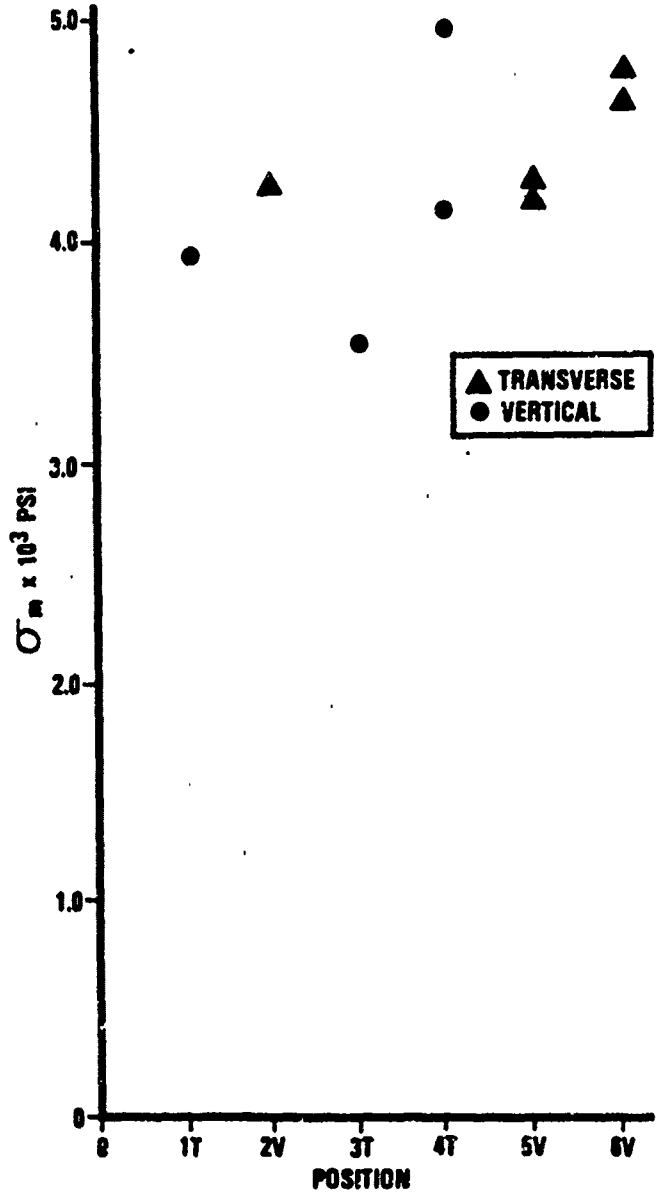

Figure 20. Compressive strength, σ_m, versus position and orientation of sample in cast for Comp B II

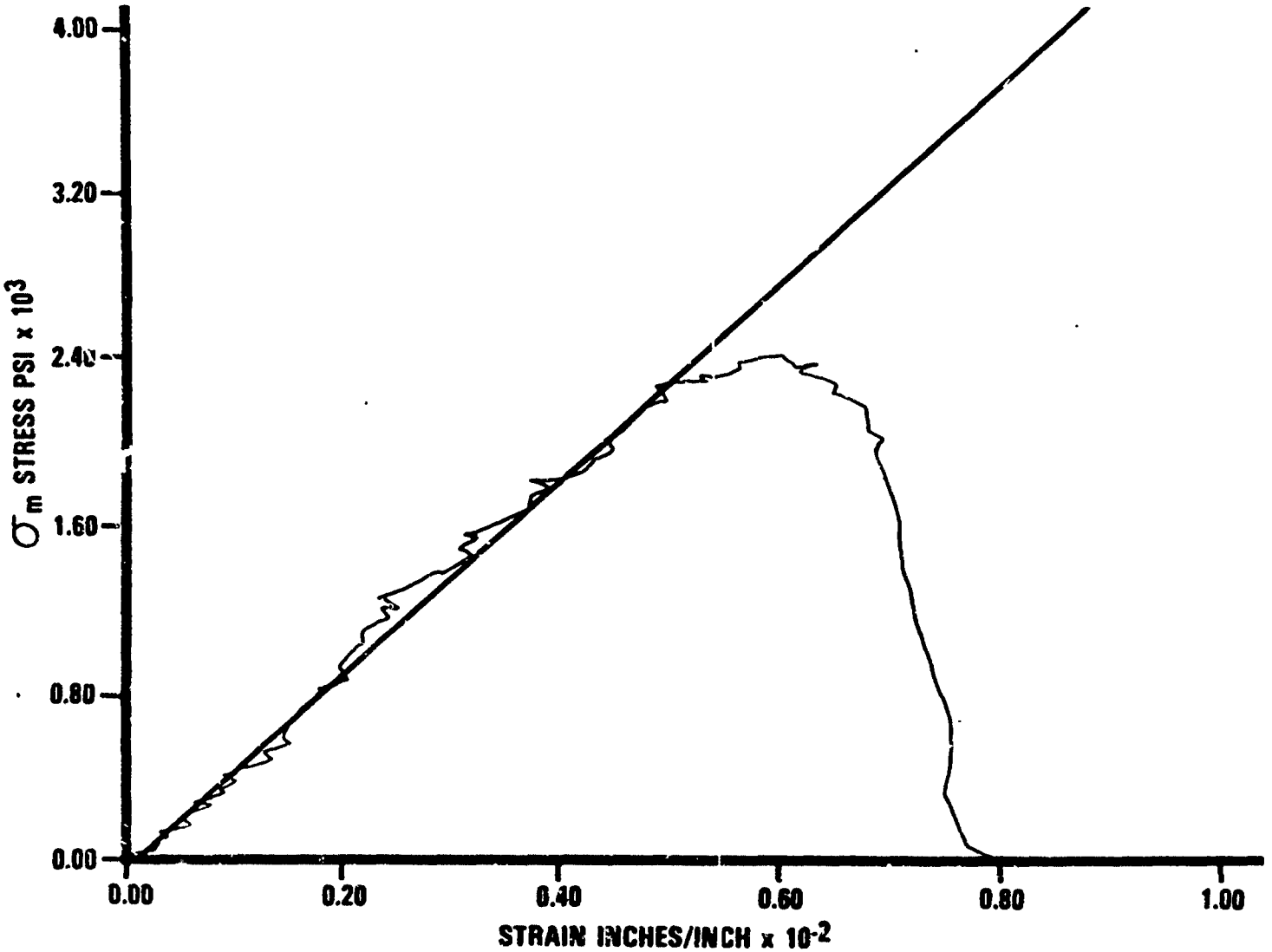

Figure 21. Typical stress, σ, versus strain, ε, curve for TNT showing the determination of the modulus E. E is taken as the slope of the straight line part of the

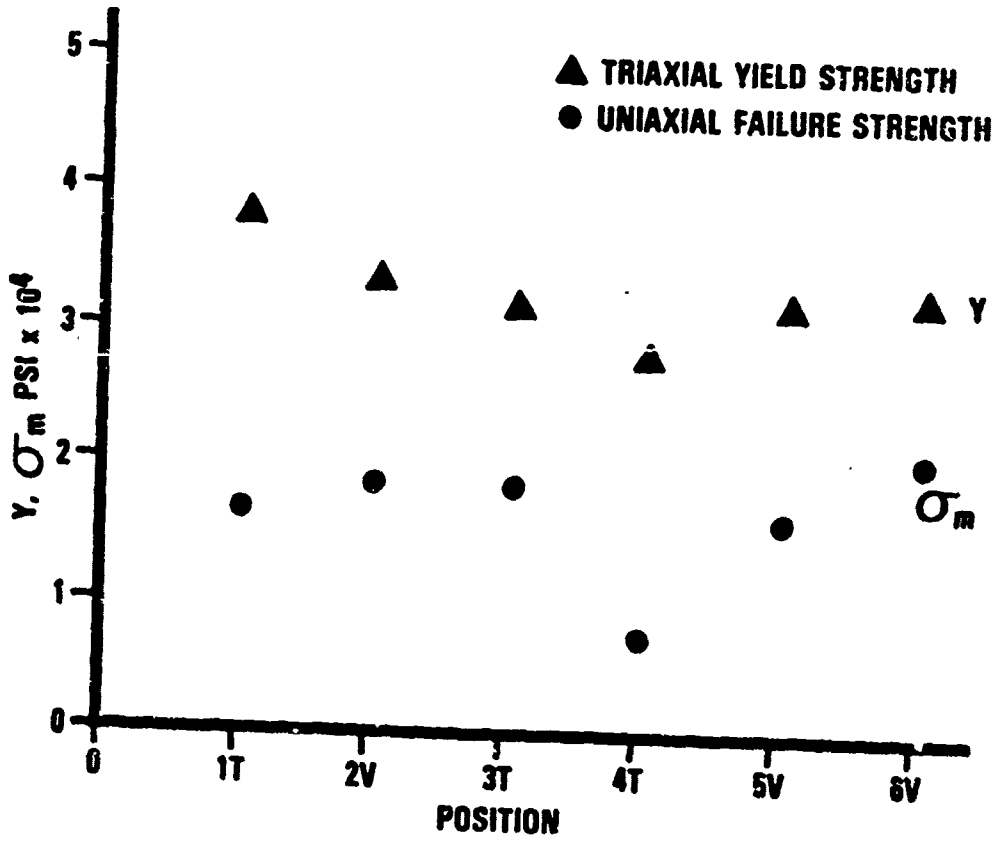

Figure 22. Compressive strength, σ_m, and the yield strength, Y, versus position and orientation of sample in cast for TNT - high strain rate

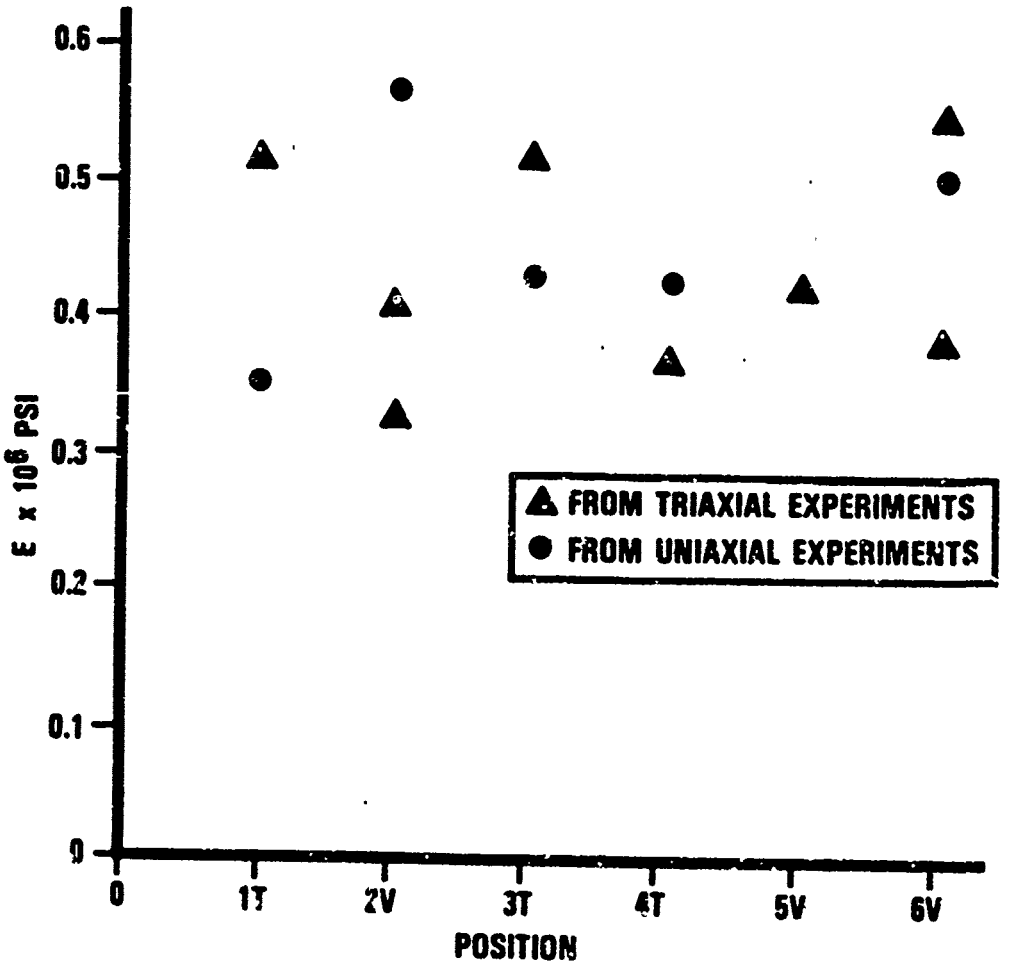

Figure 23. Young's modulus, E, versus position and orientation of sample in cast for TNT, uniaxial and triaxial data - high strain rate

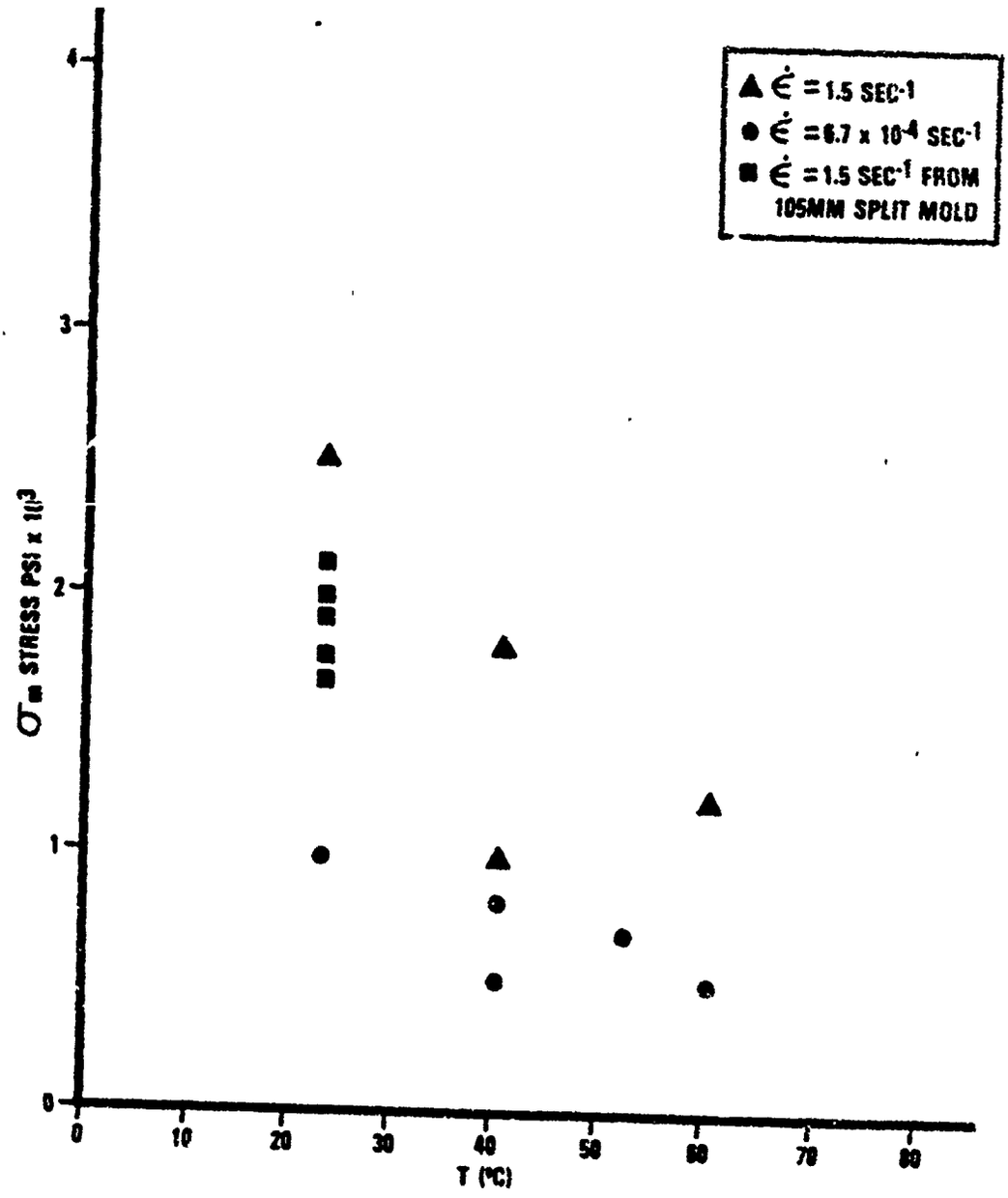

Figure 24. Compressive strength, σ_m, versus temperature for TNT for low and high strain rates

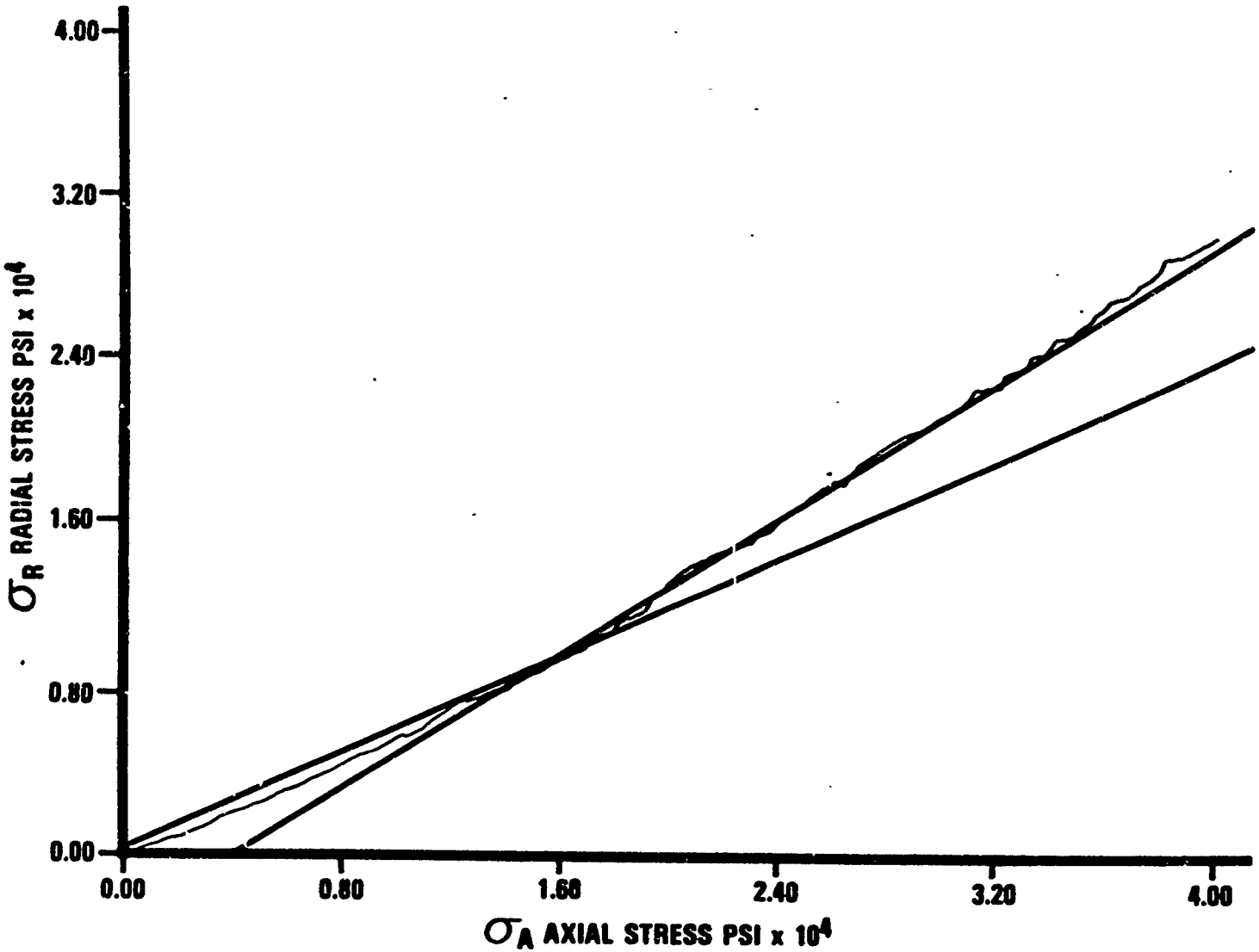

Figure 25. Typical radial stress, σ_R, versus axial stress, σ_A, for TNT for confined cylinder geometry showing linear elastic and linear plastic ranges

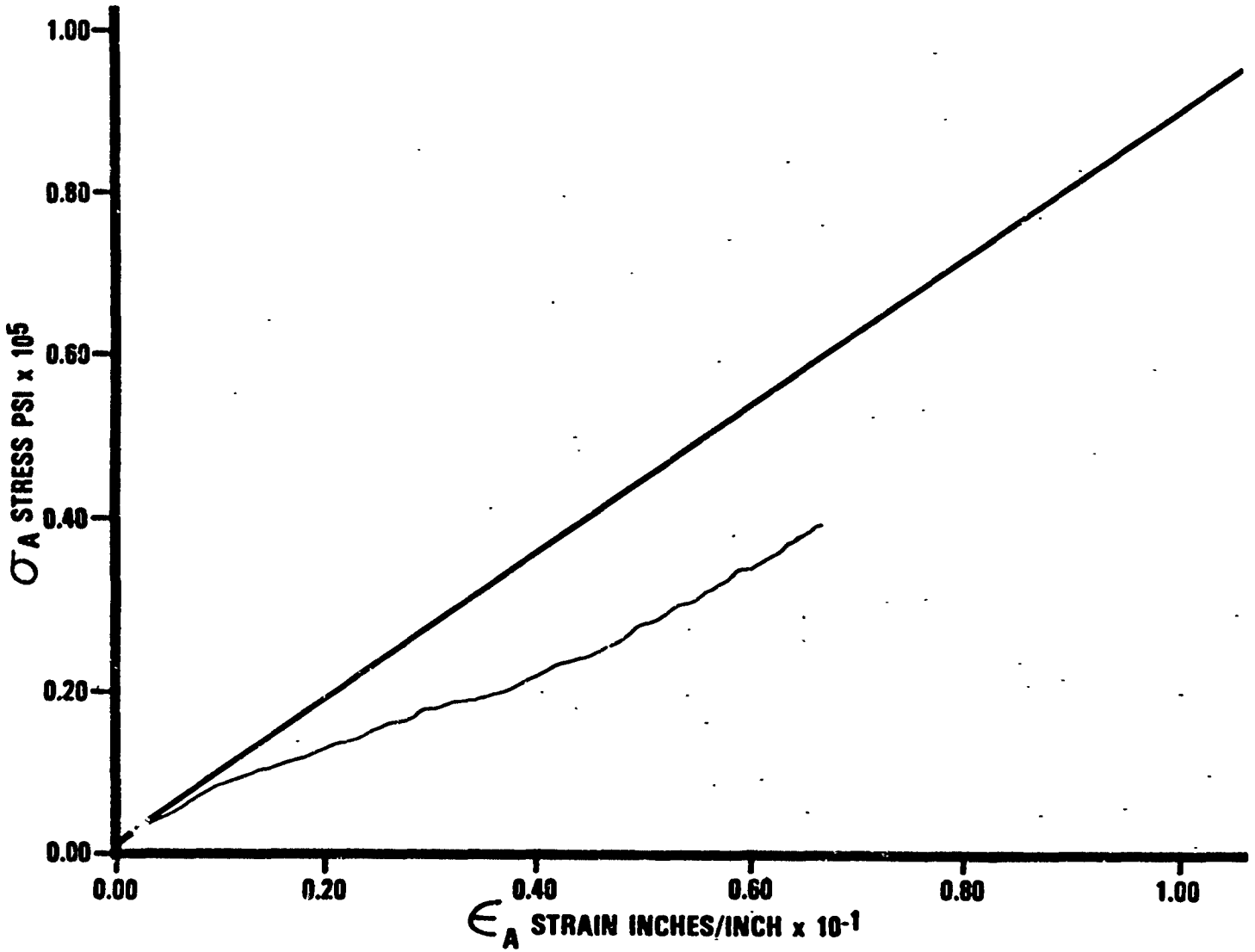

Figure 26. Typical axial stress, σ_A, versus axial strain, ϵ_A, for TNT for the confined cylinder geometry

Consider a cylindrical sample with graphite on the surfaces and confined by a steel cylinder. Assume a coefficient of friction between the steel and the specimen $f \ll 1$. Further assume that symmetry exists about the mid plane as indicated below.

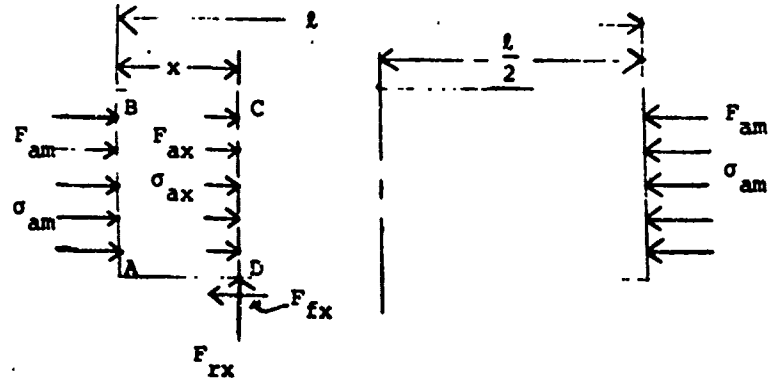

Consider a slab of specimen at one end of thickness x as indicated in the figure. The frictional forces are designated as F_{fx} and are a function of the distance x from the end. Because of the frictional forces the axial and radial forces will also be a function of this distance x. Consideration of the slab as a free body gives directly

$$F_{am} - F_{ax} = \sum F_{fx} = \int_0^x \sigma_{fx}\, 2\pi r\, dx.$$

where F_{am} and σ_{am} are the force and stress at the end, F_{ax} and σ_{ax} are the force and stress at the position x and F_{fx} and σ_{fx} are the force and stress resulting from friction at position x.

But

$$f = \frac{F_{fx}}{F_{rx}} = \frac{\sigma_{fx}}{\sigma_{rx}}$$

where F_{rx} and σ_{rx} are the force and stress in the radial direction at position x.

In the elastic range

$$\sigma_{rx} = k\sigma_{ax}$$

so that $\sigma_{fx} = f\sigma_{rx} = fk\sigma_{ax}$

and

$$F_{am} - F_{ax} = 2\pi rfk \int_0^x \sigma_{ax} dx$$

$$\sigma_{am} - \sigma_{ax} = \frac{2\pi rfk}{\pi r^2} \int_0^x \sigma_{ax} dx$$

$$= \frac{2fk}{r} \int_0^x \sigma_{ax} dx$$

and differentiating

$$-d\sigma_{ax} = \frac{2fk}{r} \sigma_{ax} dx$$

which leads to

$$\frac{\sigma_{ax}}{\sigma_{fm}} = \epsilon^{\frac{-2fk}{r} x}$$

and

$$\sigma_{a\frac{\ell}{2}} = \sigma_{am} \; \epsilon^{\frac{-\ell fk}{r}} \qquad x = \frac{\ell}{2}$$

$$\sigma_{a\frac{\ell}{2}} = \sigma_{am} \; \epsilon^{-2fk} \qquad \ell = 2r$$

$$= \frac{\sigma_r \frac{\ell}{2}}{k}$$

so

$$\sigma_r \frac{\ell}{2} = k \, \epsilon^{-2fk} \, \sigma_{am} .$$

This is the desired quanity because measurements are made of $\sigma_{r\ell}$ and σ_{am}. Because of friction the slope of the $\sigma_{r\ell}$ versus σ_{am} curve is decressed by the factor ϵ^{-2fk}. This factor approaches unity as $f \to o$.

In the yield region the relationship of σ_{ax} to σ_{rx} is given by the von Mises condition.

$$\sigma_{ax} - \sigma_{rx} = Y$$

$$\sigma_{fx} = f\sigma_{rx} = f\,[\sigma_{ax} - Y]$$

and again by equating forces

$$F_{am} - F_{ax} = 2\pi f r \int_o^x (\sigma_{ax} - Y)dx$$

and

$$\sigma_{am} - \sigma_{ax} = \frac{2f}{r} \int_o^x (\sigma_{ax} - Y)dx \,.$$

By taking derivatives

$$- d\sigma_{ax} = \frac{2f}{r} (\sigma_{ax} - Y)\, dx$$

Let

$$\sigma'_{ax} = \sigma_{ax} - Y$$

$$d\sigma'_{ax} = d\sigma_{ax}$$

and so

$$- d\sigma'_{ax} = \frac{2f}{r} \sigma'_{ax}\, dx$$

$$\frac{\sigma'_{ax}}{\sigma'_{am}} = \varepsilon^{\frac{-2f}{r}x}$$

and

$$\frac{\sigma_{ax} - Y}{\sigma_{am} - Y} = \varepsilon^{\frac{-2fx}{r}}$$

$$\sigma_{ax} = Y + (\sigma_{am}-Y)\ \varepsilon^{\frac{-2fx}{r}}$$

and

$$\sigma_{a\frac{\ell}{2}} = Y + (\sigma_{am}-Y)\ \varepsilon^{\frac{-2f\ell}{2r}}$$

and if

$$\ell = 2r$$

$$\sigma_{a\frac{\ell}{2}} = Y + (\sigma_{am}-Y)\ \varepsilon^{-2f}$$

and from

$$Y = \sigma_{a\frac{\ell}{2}} - \sigma_{r\frac{\ell}{2}}$$

$$Y = Y + (\sigma_{am} - Y)\ \varepsilon^{-2f} - \sigma_{r\frac{\ell}{2}}$$

$$\sigma_{am}\ \varepsilon^{-2f} - \sigma_{r\frac{\ell}{2}} = Y\ \varepsilon^{-2f}$$

which is of the form

$$\sigma_{am}S - \sigma_{r\frac{\ell}{2}} = B = YS\ .$$

This is the same form as the experimental relationship. In particular for the intercept when

$$\sigma_{r\frac{\ell}{2}} = 0$$

$$\sigma_{an} S = YS$$

$$\sigma_{an} = Y$$

Further, the slope is

$$S = \varepsilon^{-2f}$$

which is less than one but approaches unity as friction goes to zero.

DISTRIBUTION LIST

Commander
Armament Research and Development Center
U.S. Army Armament, Munitions, and Chemical Command
ATTN: SMCAR-FS P. Marinkas
SMCAR-FSA-E C. Larson
SMCAR-AEE (3)
SMCAR-AEE-WE B. Fishburn
D. Wiegand (15)
J. Pinto
S. Nicolaides
M. Mezger
Y. Lanzerotti
SMCAR-AEE-WW N. Slagg
R. Velicky
O. Klamer
R. Graybush
SMCAR-MSI (5)
Dover, NJ 07801-5001

Commander
U.S. Army Armament, Munitions and Chemical Command
ATTN: AMSMC-GCL(D)
Dover, NJ 07801-5001

Administrator
Defense Technical Information Center
ATTN: Accessions Division (2)
Cameron Station
Alexandria, VA 22304-6145

Director
U.S. Army Materiel Systems Analysis Activity
ATTN: AMXSY-D
AMXSY-MP
Aberdeen Proving Ground, MD 21005-5066

Commander
Armament Research and Development Center
U.S. Army Armament, Munitions and Chemical Command
ATTN: AMSMC-QAR-R, L. Manoie
E. Bixon
Dover, NJ 07801-5001

Commander
Chemical Research and Development Center
U.S. Army Armament, Munitions and Chemical Command
ATTN: SMCCR-SPS-IL
Aberdeen Proving Ground, MD 21010-5423

Commander
Chemical Research and Development Center
U.S. Army Armament, Munitions and Chemical Command
ATTN: SMCCR-RSP-A
Aberdeen Proving Ground, MD 21010-5423

Director
Ballistic Research Laboratory
ATTN: AMXBR-BLC, Mr. Starkenberg
AMXBR-BLT, Mr. Frey
Dr. Howe
AMXBR-OD-ST
Aberdeen Proving Ground, MD 21005-5066

Chief
Benet Weapons Laboratory, CCAC
Armament Research and Development Center
U.S. Army Armament, Munitions and Chemical Command
ATTN: SMCAR-CCB-TL
SMCAR-LCB-RA J. Vasilakis
Watervliet, NY 12189-5000

Commander
U.S. Army Armament, Munitions and Chemical Command
ATTN: SMCAR-ESP-L
Rock Island, IL 61299-6000

Director
U.S. Army TRADOC Systems Analysis Activity
ATTN: ATAA-SL
White Sands Missile Range, NM 88002

Lawrence Livermore National Laboratory
ATTN: M.S. Costantino
L-324
PO Box 808
Livermore, CA 94550

Morton Thiokol Inc.
Louisiana Division
ATTN: Lee C. Estabrook
P.O. Box 30058
Shreveport, LA 71130

Commander
Naval Weapons Station
ATTN: L. Rothstein
Code 50 - NEDED
Yorkstown, VA 23491